parallel to the C-I-O near-linear moiety and the direction of the shorter of the two I-Cl interactions, respectively, for these two compounds. The difference implies an I-O bond order of 0.27, assuming that the two I-C bonds contribute equivalently to the I p_x and p_y orbitals, respectively. This compares well with the value of 0.295 derived from the interatomic separation discussed above. Such agreement, which may well be somewhat fortuitous in view of the assumptions implied, does suggest that further studies correlating bond valence parameters with Mössbauer data may help in the understanding of the nature and order of secondary bonds in iodine(III) and related species.

Acknowledgment. We thank the Natural Sciences and Engineering Research Council of Canada for providing operating grants (to T.B.) and an equipment grant for the diffractometer and Dr. J. W. Harvey and M. P. Butler of the McMaster Reactor Facility for help with the neutron irradiations.

Registry No. $Ca_3{}^{127}TeO_6$, 101419-02-7; TeO_2, 7446-07-3; CaO, 1305-78-8; Ca_3TeO_6, 20354-81-8; I_2, 7553-56-2; diphenyliodonium-2-carboxylate hydrate, 96195-89-0.

Supplementary Material Available: Tables VI and VII, containing anisotropic thermal parameters and final structure factor amplitudes (15 pages). Ordering information is given on any current masthead page.

Contribution from the Laboratoire de Chimie de Coordination du CNRS, Unité No. 8241 liée par convention à l'Université Paul Sabatier, 31400 Toulouse, France, and School of Chemical Sciences, University of Illinois, Urbana, Illinois 61801

Manganese(II) Complexes of Polydentate Schiff Bases. 1. Synthesis, Characterization, Magnetic Properties, and Molecular Structure

Bouchra Mabad,[1a] Patrick Cassoux,[1a] Jean-Pierre Tuchagues,*[1a] and David N. Hendrickson*[1b]

Received September 17, 1985

The synthesis, infrared spectra, EPR, and variable-temperature magnetic susceptibility of 13 manganese(II) complexes with Schiff base ligands are described. These potentially penta- or hexadentate Schiff base ligands include N_2O_3, N_3O_2, and N_4O_2 donor sets and result from the condensation of salicylaldehyde, or 5-nitrosalicylaldehyde, with diaminopropanol or tri- or tetraamines. The crystal molecular structure of Mn^{II}[5-NO_2-sal-N(1,5,9,13)]·0.65$C_2H_4Cl_2$ has been established by X-ray diffraction methods. This complex crystallizes in the orthorhombic space group D_{2h}^6-*Pnna* in a cell of dimensions a = 20.732 (4) Å, b = 16.906 (2) Å, and c = 15.861 (3) Å, with Z = 8. The structure was solved by the heavy-atom method and refined by a full-matrix least-squares technique to conventional agreement indices R = 0.038 and R_w = 0.041 with 2208 unique reflections for which $F_o^2 > \sigma(F_o^2)$. The results obtained provide evidence that all manganese(II) complexes described here are high-spin penta- or hexacoordinated species. Minor changes in the design of the polydentate ligands result in different architectural arrangements of the corresponding complexes: Mn^{II}(saldpt) and Mn^{II}(5-NO_2-saldpt), characterized by the N_3O_2 ligand donor set with propylene units bridging the three N atoms, are monomeric. Also monomeric are Mn^{II}(salaep)$_2$ and Mn^{II}(5-NO_2-salaep)$_2$, both of which have two tridentate N_2O ligands, and Mn^{II}[sal-N(1,4,7,10)], Mn^{II}[5-NO_2-sal-N(1,4,7,10)], Mn^{II}[sal-N(1,5,8,12)], Mn^{II}[5-NO_2-sal-N(1,5,8,12)], Mn^{II}[sal-N-(1,5,9,13)], and Mn^{II}[5-NO_2-sal-N(1,5,9,13)], which incorporate hexadentate N_4O_2 ligands. Mn^{II}(saldien), which has a N_3O_2 donor set ligand with ethylene bridges between the three nitrogen atoms, is a dimer. Mn^{II}(salprenOH), which has a N_2O_3 donor set ligand with an alcoholic function between the two imine nitrogen atoms, exhibits a structure with extended intermolecular magnetic exchange interactions in the solid state. Mn^{II}(5-NO_2-saldien) exhibits weak extended intermolecular interactions in the solid state and is a dimer when dissolved in noncoordinating solvents. IR and EPR data indicate the presence of cis and trans isomers with respect to the phenolic oxygen atoms for all monomeric complexes. The dimeric complexes behave as spectral analogues for the active site of the photosynthetic water-splitting enzyme.

Introduction

Manganese is of industrial and biological importance. Manganese(III) is known to oxidize alkylbenzenes, alcohols, carboxylic acids, phenols, and ethers.[2] The site where oxidation of water gives dioxygen in photosynthesis[3] and the electron-transfer reaction of mitochondrial superoxide dismutase[4] both involve manganese ions. The role that manganese plays in all these processes is undoubtedly related to the ability of the manganese ion to function as a redox catalyst.[5] The capacity of the metal ion to change between oxidation states can be related to metal-metal interactions (binuclear and multi-metal-centered catalysts)[6] and/or to the ligand field produced about the metal ion.[7] Thus, the ligand structure that maintains the metal centers in close or remote proximity and creates the ligand field plays a key role in the oxidation-state accessibility. In this regard, the oxidation-state accessibility of manganese has been explored by using a large variety of ligands.[8]

Very little is known about the role of manganese in photosynthetic systems. In green plants and algae, although manganese is known to be at the active site of a metalloprotein that mediates the oxidation of water to molecular oxygen, its exact role and environment in the thylakoid membrane are unknown.[9] The stoichiometry requirement of manganese for O_2 evolution in active thylakoid membranes is four[10] per center. The oxidation state of these manganese ions is thought to vary through the five Kok cycle states[3] (S_0-S_4) between 2+ and 4+.[9] EXAFS studies[11]

(1) (a) Université Paul Sabatier. (b) University of Illinois.
(2) Benson, D. *Mechanisms of Oxidation by Metal Ions*; Elsevier: New York, 1976.
(3) (a) Kok, B.; Forbush, B.; McGloin, M. *Photochem. Photobiol.* **1970**, *11*, 457-475. (b) Cheniae, G. M.; Martin, M. *Biochim. Biophys. Acta* **1970**, *197*, 219-239.
(4) Fridovich, I. *Adv. Inorg. Biochem.* **1979**, *1*, 67-91.
(5) (a) Calvin, M. *Rev. Pure Appl. Chem.* **1965**, *15*, 1-10. (b) Olson, J. M. *Science (Washington, D.C.)* **1970**, *168*, 438-446. (c) Keele, B. B.; McCord, J. M.; Fridovich, I. *J. Biol. Chem.* **1970**, *245*, 6176-6181.
(6) Muetterties, E. L. *Bull. Soc. Chim. Belg.* **1975**, *84*, 959-986 and references therein.
(7) Buckingham, D. A.; Sargeson, A. M. In *Chelating Agents and Metal Chelates*; Dwyer, F. P., Mellor, D. P., Eds.; Academic: New York, 1969.
(8) (a) Lawrence, G. D.; Sawyer, D. T. *Coord. Chem. Rev.* **1978**, *27*, 173-193. (b) Coleman, W. M.; Taylor, L. T. *Coord. Chem. Rev.* **1980**, *32*, 1-31.
(9) (a) Clayton, R. K. *Photosynthesis, Physical Mechanisms and Chemical Patterns*; IUPAB Biophysics Series; Cambridge University Press: Cambridge, 1980. (b) Govindjee. *Photosynthesis, Energy Conversion by Plants and Bacteria*; Academic: New York, 1982; Vol. 1. (c) Livorness, J.; Smith, T. D. *Struct. Bonding (Berlin)* **1982**, *48*, 2-44. (d) Amez, J. *Biochim. Biophys. Acta* **1983**, *726*, 1-12.
(10) Yocum, C. F.; Yerkes, C. T.; Blankenship, R. E.; Sharp, R. R.; Babcock, G. T. *Proc. Natl. Acad. Sci. U.S.A.* **1981**, *78*, 7507-7511.
(11) Kirby, J. A.; Robertson, A. S.; Smith, J. P.; Thompson, A. C.; Cooper, S. R.; Klein, M. P. *J. Am. Chem. Soc.* **1981**, *103*, 5529-5537.

0020-1669/86/1325-1420$01.50/0

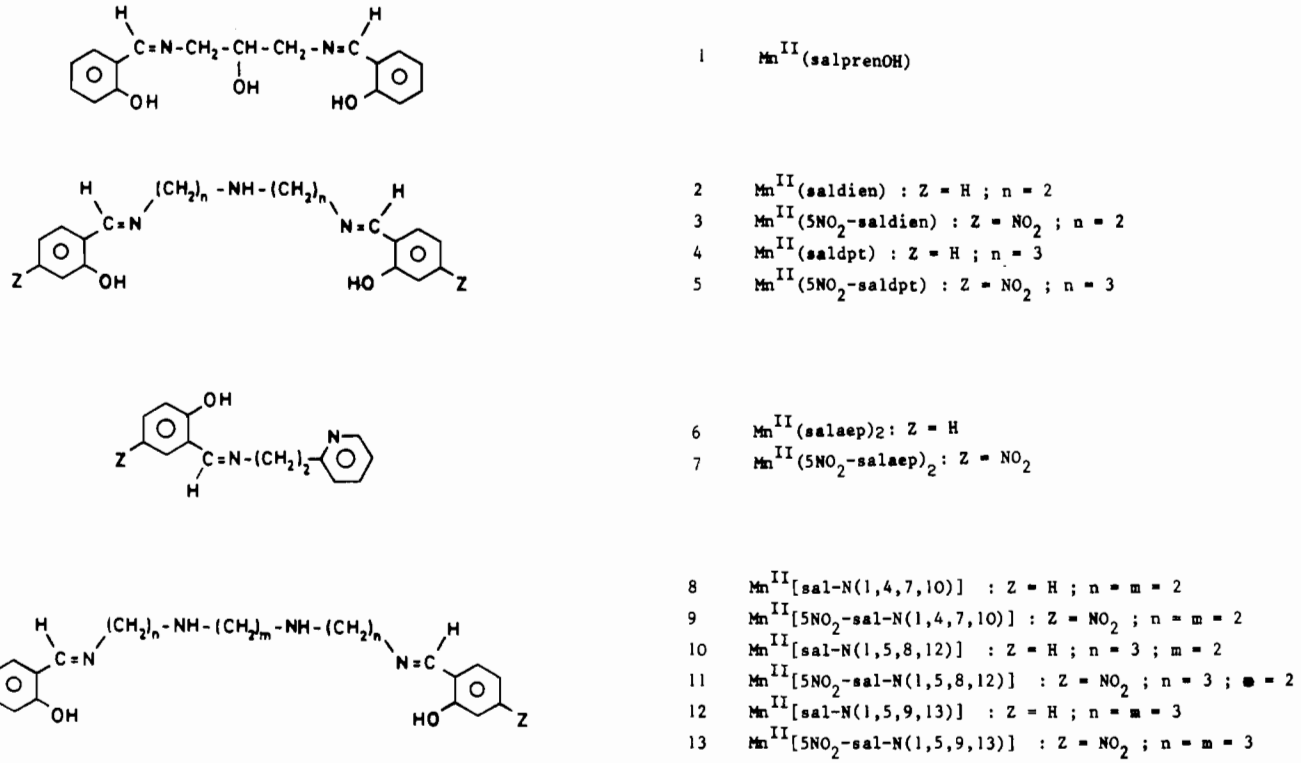

Figure 1. Schematic representation of the ligands and numbering and abbreviations of the complexes studied in this work.

suggest a Mn–Mn separation of 2.7 Å and an inner coordination sphere for manganese consisting of "light" donor atoms (O, N). Comparison of the manganese K-edge energies (XAES) of chloroplast samples with reference compounds places the average oxidation state of manganese in chloroplasts between 2+ and 3+.[12] It has been suggested that the manganese ions of the oxygen-evolving system are involved in clusters containing at least two and up to four metal centers.[13] A very recent hypothesis has been reported where a binuclear Mn^{III} site with one redox-active ligand per manganese ion oxidizes two H_2O ligands to give O_2.[14]

A few manganese complexes have been studied as coordination site models of manganese in the photosystem II of the thylakoid membranes: Schiff base complexes,[15] manganese gluconate,[16] bis(μ-oxo)-bridged binuclear manganese complexes,[17,18] manganese β-cyclodextrin complex,[19] and manganese catechol[20] and semiquinone[21] complexes.

Taylor et al.[22] have described the synthesis of manganese(II) and manganese(III) complexes with polydentate Schiff base ligands. Their results from room-temperature magnetic susceptibility measurements and electrochemical and oxygenation studies raised questions that remained unanswered, especially regarding the association state and the nature and number of accessible oxidation states.

We report here the initial results of a systematic study of Schiff base manganese complexes as models of the photosystem II manganese site. The synthesis and detailed IR, EPR, variable-temperature magnetic susceptibility, and X-ray structural determination results for a series of manganese(II) complexes with potentially penta- and hexadentate Schiff base ligands including N_2O_3, N_3O_2, and N_4O_2 donor sets (Figure 1) are reported in this paper. The results and analysis of the electrochemical studies together with an examination of the manganese(IV) complexes electrochemically generated and oxygenation studies will be presented in a subsequent paper.[23] Our goal is to obtain a description of the magnetic and electrochemical properties of these complexes detailed enough to evaluate the interest of such manganese complexes as spectral analogues for the active site of the photosynthetic water-splitting enzyme. A preliminary analysis of the relevance of some of these complexes to the oxygen-evolving site of photosystem II has already been published.[24]

Experimental Section

Materials. 1,5,9,13-Tetraazatridecane (N(1,5,9,13)) was prepared by a catalytic hydrogenation method similar to that used by Freifelder.[25] *N,N'*-Bis(2-cyanoethyl)-1,3-diaminopropane was prepared by reaction of

(12) Kirby, J. A.; Goodin, D. B.; Wydrzynski, T. W.; Robertson, A. S.; Klein, M. P. *J. Am. Chem. Soc.* **1981**, *103*, 5537–5542.
(13) (a) Dismukes, G. C.; Siderer, Y. *Proc. Natl. Acad. Sci. U.S.A.* **1981**, *78*, 274–278. (b) Dismukes, G. C.; Ferris, K. E.; Watnick, P. *Photobiochem. Photobiophys.* **1982**, *3*, 243–256. (c) Paula, J. C.; Brudvig, G. W. *J. Am. Chem. Soc.* **1985**, *107*, 2643–2648.
(14) Kambara, T.; Govindjee. *Proc. Natl. Acad. Sci. U.S.A.* **1985**, *82*, 6119–6123.
(15) (a) Boucher, L. J.; Coe, C. G. *Inorg. Chem.* **1975**, *14*, 1289–1295. (b) Boucher, L. J.; Coe, C. G. *Inorg. Chem.* **1976**, *15*, 1334–1340.
(16) (a) Sawyer, D. T.; Bodini, M. E. *J. Am. Chem. Soc.* **1975**, *97*, 6588–6590. (b) Bodini, M. E.; Willis, L. A.; Riechel, T. E.; Sawyer, D. T. *Inorg. Chem.* **1976**, *15*, 1538–1543. (c) Bodini, M. E.; Sawyer, D. T. *J. Am. Chem. Soc.* **1976**, *98*, 8366–8371.
(17) Morrison, M. M.; Sawyer, D. T. *J. Am. Chem. Soc.* **1977**, *99*, 257–258.
(18) (a) Calvin, M. *Science (Washington, D.C.)* **1974**, *184*, 375–381; **1975**, *185*, 376. (b) Cooper, S. T.; Calvin, M. *J. Am. Chem. Soc.* **1977**, *99*, 6623–6630. (c) Cooper, S. R.; Dismukes, G. C.; Klein M. P.; Calvin, M. *J. Am. Chem. Soc.* **1978**, *100*, 7248–7252.
(19) Unni Nair, B.; Dismukes, G. C. *J. Am. Chem. Soc.* **1983**, *105*, 124–125.
(20) (a) Magers, K. D.; Smith, C. G.; Sawyer, D. T. *J. Am. Chem. Soc.* **1978**, *100*, 989–991. (b) Magers, K. D.; Smith, C. G.; Sawyer, D. T. *Inorg. Chem.* **1980**, *19*, 492–496. (c) Stallings, M. D.; Morrison, M. M.; Sawyer, D. T. *Inorg. Chem.* **1981**, *20*, 2655–2660. (d) Jones, S. E.; Chin, D. H.; Sawyer, D. T. *Inorg. Chem.* **1981**, *20*, 4257–4262. (e) Cooper, S. R.; Hartman, J. R. *Inorg. Chem.* **1982**, *21*, 4315–4317.
(21) (a) Mathur, P.; Dismukes, G. C. *J. Am. Chem. Soc.* **1983**, *105*, 7093–7098. (b) Lynch, M. W.; Hendrickson, D. N.; Fitzgerald, B. J.; Pierpont, C. G. *J. Am. Chem. Soc.* **1984**, *106*, 2041–2049.
(22) (a) Coleman, W. M.; Taylor, L. T. *Inorg. Chem.* **1977**, *16*, 1114–1119. (b) Coleman, W. M.; Goehring, R. R.; Taylor, L. T.; Mason, J. G.; Boggess, R. K. *J. Am. Chem. Soc.* **1979**, *101*, 2311–2315. (c) Coleman, W. M.; Taylor, L. T. *J. Inorg. Nucl. Chem.* **1980**, *42*, 683–687. (d) Coleman, W. M.; Boggess, R. K.; Hughes, J. W.; Taylor, L. T. *Inorg. Chem.* **1981**, *20*, 700–706. (e) Coleman, W. M.; Boggess, R. K.; Hughes, J. W.; Taylor, L. T. *Inorg. Chem.* **1981**, *20*, 1253–1258. (f) Frederick, F. C.; Coleman, W. M.; Taylor, L. T. *Inorg. Chem.* **1983**, *22*, 792–795.
(23) Tuchagues, J.-P., et al., to be submitted for publication.
(24) Mabad, B.; Tuchagues, J. P.; Hwang, Y. T.; Hendrickson, D. N. *J. Am. Chem. Soc.* **1985**, *107*, 2801–2802.
(25) Freifelder, M. *J. Am. Chem. Soc.* **1960**, *82*, 2386–2389.

1,3-diaminopropane with acrylonitrile.[26] Acrylonitrile, 1,3-diaminopropane, bis(3-aminopropyl)amine (dpt), 1,4,7,10-tetraazadecane (N(1,4,7,10)), and salicylaldehyde were purchased from Aldrich or Fluka in high-purity grade and used as received. Manganese acetate tetrahydrate was obtained from Alfa Inorganics. 1,3-Diamino-2-hydroxypropane (Aldrich) and 5-nitrosalicylaldehyde (Eastman) were sublimed prior to use. 1,5,8,12-Tetraazadodecane (N(1,5,8,12)) (Strem) and 1,5,9,13-tetraazatridecane (N(1,5,9,13)) (vide supra) were fractionally distilled at 118 °C (0.2 mmHg) and 138 °C (2 mmHg), respectively. Diethylenetriamine (dien) and 2-(aminoethyl)pyridine (aep) (Aldrich) were distilled at 199 °C and 93 °C, respectively. All other chemicals were reagent grade or equivalent.

Hexane, heptane, benzene, toluene, and THF were refluxed over sodium/benzophenone and distilled under argon. Methanol and absolute ethanol were distilled under argon. Dimethylformamide was shaken over KOH for 1 h, refluxed over BaO for 30 min, and distilled under argon. The center cut (10–90%) was further distilled under vacuum. All solvents were degassed under vacuum prior to use.

Ligands. The ligands resulting from the Schiff base condensation of an amine or a polyamine with salicylaldehyde are very thick oils that were not further purified or studied. The salprenOH ligand results from the condensation of salicylaldehyde and 1,3-diamino-2-hydroxypropane as described by Dey.[27] Recrystallized from ethanol, it affords light yellow crystals. The ligands prepared from 5-nitrosalicylaldehyde were obtained as yellow to orange powders depending on the starting amine. They were washed with methanol, or absolute ethanol, and hexane. They were finally filtered off and dried under vacuum. All isolated ligands gave satisfactory analytical results.[28]

Complexes. Due to the oxygen sensitivity of these manganese(II) complexes in solution, all reactions were performed under an atmosphere of purified argon. Argon was scrubbed of O_2 by MnO columns and then passed through 3-Å predried molecular sieves to minimize the water content. Schlenk techniques were employed to prepare all the complexes. The general method of preparation was as follows. To a stirred solution of the appropriate aldehyde (10 mmol) in 20 mL of methanol was added dropwise the appropriate amine (5 mmol) dissolved in 20 mL of methanol. The reaction mixture was refluxed for 1 h and then cooled to room temperature. A 10-mmol quantity of sodium methoxide was added dropwise to the stirred ligand slurry or solution. The resulting deprotonated ligand solution was then carefully degassed under vacuum prior to the addition of an oxygen-free methanol solution containing 5 mmol of manganese acetate tetrahydrate. A yellow to orange precipitate usually formed before the end of the manganese(II) acetate addition. According to the speed and abundance of precipitate formation, the slurry was stirred for 2–18 h at temperatures ranging from 20 to 65 °C. The resulting complex was filtered off, washed with 20 mL of methanol and 20 mL of hexane, and dried under vacuum for 6 h. The complex was directly transferred and stored in an inert-atmosphere box (Jahan BS 0012) equipped with a Dri-Train (Jahan EVAC 7). Absolute ethanol could be substituted for or mixed with the methanol without modifying this synthesis. The samples thus prepared were found to be analytically purer than those prepared from ligands deprotonated with NaOH or KOH solutions. We observed that the use of nondeprotonated ligands yields reaction mixtures that need to be refluxed for 24–48 h in order to complete the reactions and often affords samples with oxidation traces. Although the ligands including the 5-NO_2 substituent could be isolated and purified, the corresponding complexes were prepared by following the one-pot reaction method described above. Samples prepared from these preformed ligands were obtained in lower yields and gave poorer analytical results. This can be attributed to the template effect of the metal ion, which drives the Schiff base condensation to completion, thus affording a better yield and preventing the presence of unreacted 5-nitrosalicylaldehyde mixed with the ligand. The analytical results for the complexes are in good agreement with the theoretical values for C, H, N, and Mn.[28]

Physical Measurements. Elemental analyses were carried out at the Laboratoire de Chimie de Coordination microanalytical laboratory in Toulouse for C, H, and N and at the Service Central de Microanalyses in Vernaison for Mn.

Infrared spectra were recorded on a 5MX Nicolet spectrophotometer coupled with a 7470A Hewlett-Packard recorder. Samples were run both as KBr pellets prepared under argon in a drybox and as Nujol mulls prepared and pressed between KBr plates under argon in a drybox.

Variable-temperature magnetic susceptibility data were obtained with a SHE 905 Squid susceptometer. Diamagnetic corrections were applied by using Pascal's constants. Least-squares computer fittings of the magnetic susceptibility data were accomplished with an adapted version of the function-minimization program STEPT.[29]

EPR spectra were obtained on a Bruker 200 TT spectrometer with magnetic field modulation at 100 kHz. The microwave frequency was generated with a Bruker ER 04 bridge for the X-band (9.3–9.4 GHz) and with a Bruker ER051QR bridge for the Q-band (33.5–34.5 GHz). The microwave frequencies were measured with a Racal-Dana frequency meter, and the magnetic field was measured with a Bruker NMR probe gaussmeter. A Bruker liquid-nitrogen cryostat was used for measurements between 100 K and room temperature. An Oxford helium cryostat was used for EPR measurements between 4 and 100 K. Solution and powdered samples were loaded in 3-mm (X-band) or 1-mm (Q-band) cylindrical quartz tubes in the drybox and then degassed and sealed under vacuum.

Table I. Summary of Crystal and Intensity Collection Data

formula	$C_{24.3}H_{30.6}N_6O_6Cl_{1.3}Mn$
mol wt	603.2
cryst syst	orthorhombic
a, Å	20.732 (4)
b, Å	16.906 (2)
c, Å	15.861 (3)
V, Å^3	5559.2
Z	8
$F(000)$	2508
D_{measd}, g·cm^{-3}	1.43 (measd by flotation in toluene/bromoform)
D_{calcd}, g·cm^{-3}	1.441
space group	D^6_{2h}-*Pnna*
radiation	Mo Kα from graphite monochromator
λ, Å	0.71069
linear abs coeff, cm^{-1}	6.28
temp, °C	20
receiving aperture, mm	4.0 × 4.0
takeoff angle, deg	4
scan mode	θ–2θ
scan range, deg	0.85 + 0.35 tan θ
2θ limits, deg	54

Structure Determination of Mn^{II}[5-NO_2-sal-N(1,5,9,13)]·0.65$C_2H_4Cl_2$. Collection and Reduction of X-ray Data. Crystals of complex **13** were obtained from a 1,2-dichloroethane solution in the form of the $C_2H_4Cl_2$ solvate. These crystals belong to the orthorhombic system, space group D^6_{2h}-*Pnna*. The selected crystal was an orange parallelepiped of approximate dimensions 0.35 × 0.30 × 0.20 mm. It was sealed on a glass fiber and mounted on an Enraf-Nonius CAD4 diffractometer. Cell constants were obtained from a least-squares fit of 25 reflections. Crystal and intensity collection data are summarized in Table I. A total of 5654 independent reflections were recorded to a 2θ (Mo) maximum of 54° by procedures described elsewhere.[30] Intensity standards, recorded periodically, showed only random, statistical fluctuations. Reflections were corrected for Lorentz and polarization effects,[31] 2208 of which with $I > \sigma(I)$, based on counting statistics, were used in subsequent calculations. No absorption corrections were made.

Structure Solution and Refinement. The structure was solved by the heavy-atom method.[32] Difference Fourier maps and the least-squares refinement cycle process revealed the positions of all non-hydrogen atoms of the molecule and the presence of residual peaks located on the special positions (4d) and (4c) and around them. These residual peaks were considered as being a trace of the crystallization solvent, i.e. 1,2-dichloroethane. Their occupancy factors were first refined and then kept fixed to 0.65 and 0.35 for atoms in general position and in special position, respectively. The calculated density (1.441 g·cm^{-3}) was then in agreement with that measured (1.43 g·cm^{-3}). These atoms were refined isotropically.

All non-hydrogen atoms of the Mn^{II}[5-NO_2-sal-N(1,5,9,13)] molecule were refined anisotropically. The hydrogen atoms were located on a difference Fourier map and introduced in calculations in constrained geometry (C–H = N–H = 0.97 Å) with temperature factors kept fixed, U_H = 0.076 Å^2.

(26) Adams, R.; Bachmann, W. E.; Blatt, A. H.; Fieser, L. F.; Johnson, J. R.; Snyder, H. R. *Org. React. (N.Y.)* **1949**, *5*, 82.
(27) Dey, K. *Z. Anorg. Allg. Chem.* **1970**, *376*, 209–213.
(28) Supplementary material.
(29) Chandler, J. P. Program 66, Quantum Chemistry Program Exchange, Indiana University.
(30) Mosset, A.; Bonnet, J.-J.; Galy, J. *Acta Crystallogr., Sect. B: Struct. Crystallogr. Cryst. Chem.* **1977**, *B33*, 2639–2644.
(31) Frentz, B. A. *SDP—Structure Determination Package*; Enraf-Nonius: Delft, 1982.
(32) Sheldrick, G. M. *SHELX76. Program for Crystal Structure Determination*; University of Cambridge: Cambridge, England, 1976.

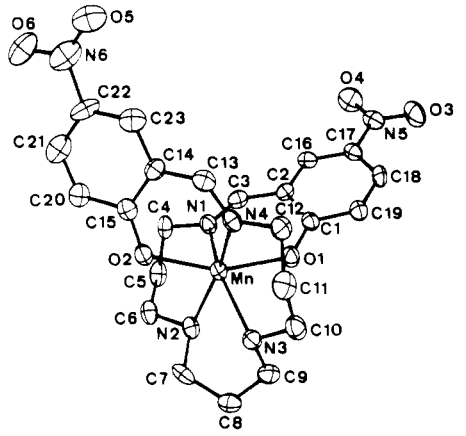

Figure 2. ORTEP view of the $Mn^{II}[5\text{-}NO_2\text{-}sal\text{-}N(1,5,9,13)]$ molecule.

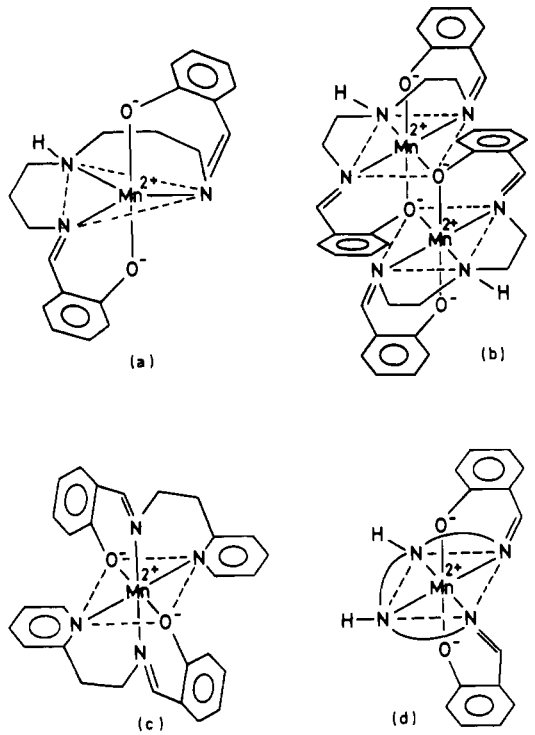

Figure 3. Coordination geometry types proposed for the studied complexes: (a) complexes **2** (solid state and solution) and **3** (solution); (b) complexes **4** and **5** (solid state); (c) complexes **6** and **7**; (d) complexes **8–13**.

The atomic scattering factors used were those proposed by Cromer and Waber[33] with anomalous dispersion effects.[34] Scattering factors for the hydrogen atoms were those of Stewart et al.[35]

The final full-matrix least-squares refinement, minimizing $\sum w(|F_o| - |F_c|)^2$, converged to $R = \sum||F_o| - |F_c||/\sum|F_o| = 0.038$ and $R_w = [\sum w(|F_o| - |F_c|)^2/\sum w|F_o|^2]^{1/2} = 0.041$ with unit weights. The goodness of fit was $S = 2.3$ with 2208 observations and 345 variables. An analysis of variance with parity groups showed larger values for those corresponding to $h + l = 2n$ (4d) and $h + k + l = 2n$ (4c). It can be attributed to the poorly refined crystallization solvent atoms. Parameter shifts were less than 0.06σ for $Mn^{II}[5\text{-}NO_2\text{-}sal\text{-}N(1,5,9,13)]$ atoms and 0.8σ for dichloroethane atoms. A final difference Fourier map showed no excursion of electron density greater than 0.4 e/Å^3. All calculations were performed on a VAX-11/730 DEC computer. The $Mn^{II}[5\text{-}NO_2\text{-}sal\text{-}N(1,5,9,13)]$ molecule is shown in Figure 2 with atom numbering. Final fractional atomic coordinates with their estimated standard deviations are given in Table II.

Table II. Fractional Atomic Coordinates of Non-Hydrogen Atoms for $Mn^{II}[5\text{-}NO_2\text{-}sal\text{-}N(1,5,9,13)]\cdot 0.65C_2H_4Cl_2$ with Estimated Standard Deviations in Parentheses

atom	x/a	y/b	z/c
Mn	0.48330 (4)	0.51762 (5)	0.68100 (5)
O(1)	0.5360 (2)	0.5350 (2)	0.7933 (2)
O(2)	0.4142 (2)	0.5425 (2)	0.5815 (2)
O(3)	0.5199 (3)	0.6739 (3)	1.1556 (3)
O(4)	0.4185 (3)	0.6431 (3)	1.1370 (3)
O(5)	0.2647 (3)	0.8610 (4)	0.6109 (4)
O(6)	0.1938 (2)	0.7869 (3)	0.5534 (3)
N(1)	0.4005 (2)	0.5068 (3)	0.7742 (3)
N(2)	0.4625 (2)	0.3858 (3)	0.6617 (3)
N(3)	0.5861 (2)	0.4922 (3)	0.6199 (3)
N(4)	0.5052 (2)	0.6468 (3)	0.6545 (3)
N(5)	0.4750 (3)	0.6477 (3)	1.1119 (3)
N(6)	0.2474 (3)	0.7978 (5)	0.5839 (5)
C(1)	0.5201 (3)	0.5637 (3)	0.8659 (3)
C(2)	0.4547 (3)	0.5634 (3)	0.8983 (3)
C(3)	0.4011 (3)	0.5270 (3)	0.8523 (4)
C(4)	0.3408 (3))	0.4681 (4)	0.7457 (4)
C(5)	0.3520 (3)	0.3814 (4)	0.7256 (4)
C(6)	0.3926 (3)	0.3663 (4)	0.6486 (4)
C(7)	0.5024 (3)	0.3572 (3)	0.5902 (3)
C(8)	0.5726 (3)	0.3429 (3)	0.6154 (4)
C(9)	0.6045 (3)	0.4144 (4)	0.6551 (4)
C(10)	0.6362 (3)	0.5502 (4)	0.6407 (4)
C(11)	0.6200 (3)	0.6342 (4)	0.6131 (4)
C(12)	0.5710 (3)	0.6760 (3)	0.6702 (4)
C(13)	0.4621 (3)	0.6972 (4)	0.6377 (4)
C(14)	0.3954 (3)	0.6799 (4)	0.6146 (4)
C(15)	0.3762 (3)	0.6025 (4)	0.5836 (4)
C(16)	0.4420 (3)	0.5898 (3)	0.9782 (3)
C(17)	0.4913 (3)	0.6223 (3)	1.0269 (3)
C(18)	0.5537 (3)	0.6275 (3)	0.9972 (4)
C(19)	0.5674 (3)	0.5991 (3)	0.9182 (4)
C(20)	0.3114 (3)	0.5963 (4)	0.5523 (4)
C(21)	0.2704 (3)	0.6569 (5)	0.5507 (4)
C(22)	0.2901 (3)	0.7311 (4)	0.5818(5)
C(23)	0.3514 (3)	0.7414 (4)	0.6127 (4)
Cl(1)	3/4	0	0.5470 (4)
C(24)	0.7367 (8)	0.0419 (9)	0.6391 (10)
C(25)	0.7439 (8)	0.1294 (9)	0.6318 (9)
Cl(2)	0.7063 (2)	0.1858 (3)	0.7028 (3)
C(26)	0.7622 (12)	1/4	3/4
C(27)	0.8028 (21)	0.2089 (24)	0.8074 (21)

Results and Discussion

As will be thoroughly discussed in this section, the experimental results indicate that the 13 complexes studied in this paper have different coordination geometry types. Figure 3 gives a schematic representation of the postulated or evidenced geometries. Extended solid-state interactions are postulated for complex **1**. A dimeric structure has been evidenced for complex **2** in the solid state and in solution, as well as for complex **3** in solution. We postulate a structure of the type in Figure 3a for these dimers. Complexes **4** and **5** are monomers with axial type geometries in the solid state (Figure 3b for example). Monomeric structures of the type in Figure 3c for complexes **6** and **7** and of the type in Figure 3d for complexes **8–13** are proposed. These complexes have a distorted octahedral geometry, as further evidenced by an X-ray molecular structure determination (Figure 2) in the case of complex **13**.

Analytical Results and Infrared Spectroscopy. Manganese(II) complexes of potentially tridentate (N_2O), pentadentate (N_2O_3 and N_3O_2), and hexadentate (N_4O_2) ligands have been prepared. On the basis of elemental analysis data,[28] compounds **1–5** and **8–13**, resulting from the reaction of Mn(II) with potentially pentadentate or hexadentate ligands, have the general formula $Mn^{II}L\cdot x$(solvent) ($x = 0, 1, 2$) while compounds **6** and **7**, resulting from the reaction of manganese(II) with potentially tridentate ligands, have the general formula $Mn^{II}L'_2\cdot x$(solvent) ($x = 0, 1, 2$). It is well-known[36] that the degree of solvation in manganese

(33) Cromer, D. T.; Waber, J. T. In *International Tables for X-ray Crystallography*; Ibers, J. A., Hamilton, W. C. Eds.; Kynoch: Birmingham, England, 1974; Vol. IV, Table 2.2.B, pp 99–101.
(34) Cromer, D. T. *Ibid.*, Table 2.3.1, p 149.
(35) Stewart, R. F.; Davidson, E. R.; Simpson, W. T. *J. Chem. Phys.* **1965**, *42*, 3175–3187.
(36) Butler, K. D.; Murray, K. S.; West, B. O. *Aust. J. Chem.* **1971**, *24*, 2249–2256.

Table III. Selected Infrared Data (cm^{-1}) for the Isolated Schiff Base Ligands

compd	ν_{OH} str	ν_{NH} str	$\nu_{C=N}$ str	ν_{NO} str	ν_{CH_2} rock	ν_{CH}(Ph) rock
salprenOH	3360 (OH + CHOH)		1650		880, 840	750
5-NO_2-saldien	3500	3345, 3320	1661	1616, 1308	942, 928, 912, 894, 863	835
5-NO_2-saldpt		3400[a]	1653	1612, 1322	902, 886, 869, 860	831
5-NO_2-salaep	3450		1662	1612, 1322	924, 892	849
5-NO_2-sal-N(1,4,7,10)		3400[a]	1652	1611, 1320	922, 893	835
5-NO_2-sal-N(1,5,8,12)		3400[a]	1663	1613, 1326	943, 905, 896, 888	840
5-NO_2-sal-N(1,5,9,13)		3400[a]	1659	1612, 1318	920, 912, 891, 876	836

[a] Very broad.

Table IV. Selected Infrared Data (cm^{-1}) for the Manganese(II) Complexes

no.	compd	ν_{OH} str	ν_{NH} str	$\nu_{C=N}$ str	ν_{NO_2} str	ν_{CH_2} rock	ν_{CH}(Ph) rock	ν_{MnO} str
1	Mn^{II}(salprenOH)	3247		1631		900, 857	761	515
2	Mn^{II}(saldien)		3341, 3294	1628		945, 924, 914, 894, 877, 853	757	505
3	Mn^{II}(5-NO_2-saldien)·CH_3OH	3439 (CH_3OH)	3312	1638	1597, 1308	922, 912	835	494
4	Mn^{II}(saldpt)·$2H_2O$	3424 (H_2O)	3247, 3200	1645		931, 910, 888, 882, 859	761	519
5	Mn^{II}(5-NO_2-saldpt)		3251	1631	1598, 1313	951, 912	839	502
6	Mn^{II}(salaep)$_2$·$2H_2O$	3420 (H_2O)		1616		906, 871	839	500
7	Mn^{II}(5-NO_2-salaep)$_2$			1627	1600, 1300	943, 908, 892, 877	780 (py), 837 (Ph)	492
8	Mn^{II}[sal-N(1,4,7,10)]·$^3/_2CH_3OH$	3310 (CH_3OH)	3295, 3233	1632		933, 916, 904, 892, 855, 846	755	508
9	Mn[5-NO_2-sal-N(1,4,7,10)]		3323, 3303	1644	1597, 1308	975, 965, 953, 929, 896, 873	844	
10	Mn^{II}[sal-N(1,5,8,12)]		3245, 3233	1628		924, 908, 844, 861, 851, 842	766	506
11	Mn^{II}[5-NO_2-sal-N(1,5,8,12)]		3266	1635	1598, 1306	952, 935, 920, 908, 888, 870	833	506
12	Mn^{II}[sal-N(1,5,9,13)]		3267, 3235	1627		930, 919, 898, 890, 878, 845	760	503
13	Mn^{II}[5-NO_2-sal-N(1,5,9,13)]		3269	1629	1594, 1308	929, 918, 908, 900, 886, 871	835	500

Schiff base complexes is variable and sometimes fractional. This explains some slight differences in the formulation of some complexes previously described.[22]

Tables III and IV list some pertinent IR frequencies for the isolated ligands and the manganese(II) complexes, respectively. Comparison of these two tables allows us to conclude that the phenolic oxygen atoms and imine linkage nitrogen atoms are coordinated to the manganese ions. We tentatively assign the weak and broad frequency near 500 cm^{-1}, which is present in the complexes and lacking in the ligand spectra, to the Mn–O phenolic bond.[37,38]

Except for complexes **3**, **5**, **11**, and **13**, the spectra of all other N–H-containing complexes (**2**, **4**, **8–10**, and **12**) exhibit a doublet in the N–H stretching region (3200–3312 cm^{-1}). The occurrence of a N–H doublet can result from three possibilities: (1) the antisymmetrical stretching frequency is intense and resolved enough to be observed, (2) a mixture of isomers is present, and (3) the site symmetry in the solid state is low. For the hexacoordinated complexes **8–10** and **12**, which contain two N–H groups, another specific explanation may be a difference in coordination of these two groups.

The CH_2 rocking frequencies of the nitrogen bridging units, as expected, are observable in the 850–950-cm^{-1} region. While most of the complexes exhibiting two N–H stretching frequencies display at least five to six CH_2 frequencies, the complexes that exhibit only one N–H stretch display two to four CH_2 rocking frequencies. This result parallels House's[39] and Buckingham's[40] observations and may be indicative of the presence of several isomers for the complexes exhibiting four or more CH_2 rocking frequencies. Moreover, we observed that most of the complexes displaying both two N–H stretches and more than four CH_2 rocking frequencies exhibit a splitting of the CH_2 stretches (2840–3100 cm^{-1}) present in the parent isolated ligand.[28]

Magnetic Susceptibility and EPR Results. The magnetic susceptibility data at 300, 70, and 5 K for the compounds described in this work are summarized in Table V. The detailed data are available in the supplementary material.[28] The 13 complexes studied have effective magnetic moments per manganese ion in the range 5.75–6.30 μ_B at room temperature, indicating the high-spin nature of each complex. These results are in agreement with the room-temperature data published by Taylor et al.[22] for some of these complexes.

Table V. Effective Magnetic Moments (μ_B)

no.	compd	300 K	70 K	5 K
1	Mn^{II}(salprenOH)	5.80	5.63	3.04
2	Mn^{II}(saldien)	5.91	5.72	3.25
3	Mn^{II}(5-NO_2-saldien)·CH_3OH	5.74	5.66	4.29
4	Mn^{II}(saldpt)·$2H_2O$	5.93	5.90	5.56
5	Mn^{II}(5-NO_2-saldpt)	6.09	6.08	5.57
6	Mn^{II}(salaep)$_2$·$2H_2O$	5.85	5.87	5.34
7	Mn^{II}(5-NO_2-salaep)$_2$	5.98	5.98	5.69
8	Mn^{II}[sal(1,4,7,10)]·$^3/_2CH_3OH$	6.31	6.28	5.87
9	Mn^{II}[5-NO_2-sal(1,4,7,10)]	6.00	5.98	5.62
10	Mn^{II}[sal-N(1,5,8,12)]	5.91	5.91	5.37
11	Mn^{II}[5-NO_2-sal-N(1,5,8,12)]	6.03	6.01	5.73
12	Mn^{II}[sal-N(1,5,9,13)]	5.91	5.91	5.58
13	Mn^{II}[5-NO_2-sal-N(1,5,9,13)]	6.30	6.28	5.90

Mn^{II}(saldpt)·$2H_2O$ (4) and Mn^{II}(5-NO_2-saldpt) (5). Complexes **4** and **5**, which have N_3O_2 ligand donor sets with propylene units bridging the three nitrogen donors, exhibit X-band powder EPR spectra characterized by broad resonances with the greatest intensity resonance centered near $g = 6$ (Figure 4). Frozen-solution X-band spectra obtained for these complexes in noncoordinating solvents (CH_2Cl_2/toluene, $CHCl_3$/toluene, or $C_2H_4Cl_2$ according to the solubilities of the complexes) show similar broad features without hyperfine patterns. Similar spectra have been observed previously for axially distorted $Mn^{II}L_4X_2$ monomeric complexes (L = α-picoline; X = Br or I) and $Mn^{II}(Ph_3XO)_4Y_2$ (X = P or As; Y = ClO_4, NCS, or I) by Goodgame et al.[41] and for trigonal-bipyramidal complexes Mn^{II}[(Me_6tren)X]X (X = Br or I) by Laskowski et al.[42] Additional information can be gained from the EPR results by using the theoretical approach of Dowsing and Gibson.[43] The spectra shown in Figure 4a,b thus indicate that

(37) Nakamoto, K. *Infrared and Raman Spectra of Inorganic and Coordination Compounds*, 3rd ed.; Wiley: New York, 1978; p 207.
(38) Ferraro, J. R. *Low Frequency Vibrations of Inorganic and Coordination Compounds*; Plenum: New York, 1971.
(39) Gainsford, A. R.; House, D. A. *Inorg. Chim. Acta* **1969**, *3*, 367–372.
(40) Buckingham, D. A.; Jones, D. *Inorg. Chem.* **1965**, *4*, 1387–1392.
(41) (a) Dowsing, R. D.; Gibson, J. F.; Goodgame, M.; Hayward, P. J. *J. Chem. Soc. A* **1969**, 187–193, 1242–1249. (b) Goodgame, D. M.; Goodgame, M.; Hayward, P. J. *J. Chem. Soc. A* **1970**, 1352–1356.
(42) Laskowski, E. J.; Hendrickson, D. N. *Inorg. Chem.* **1978**, *17*, 457–470.

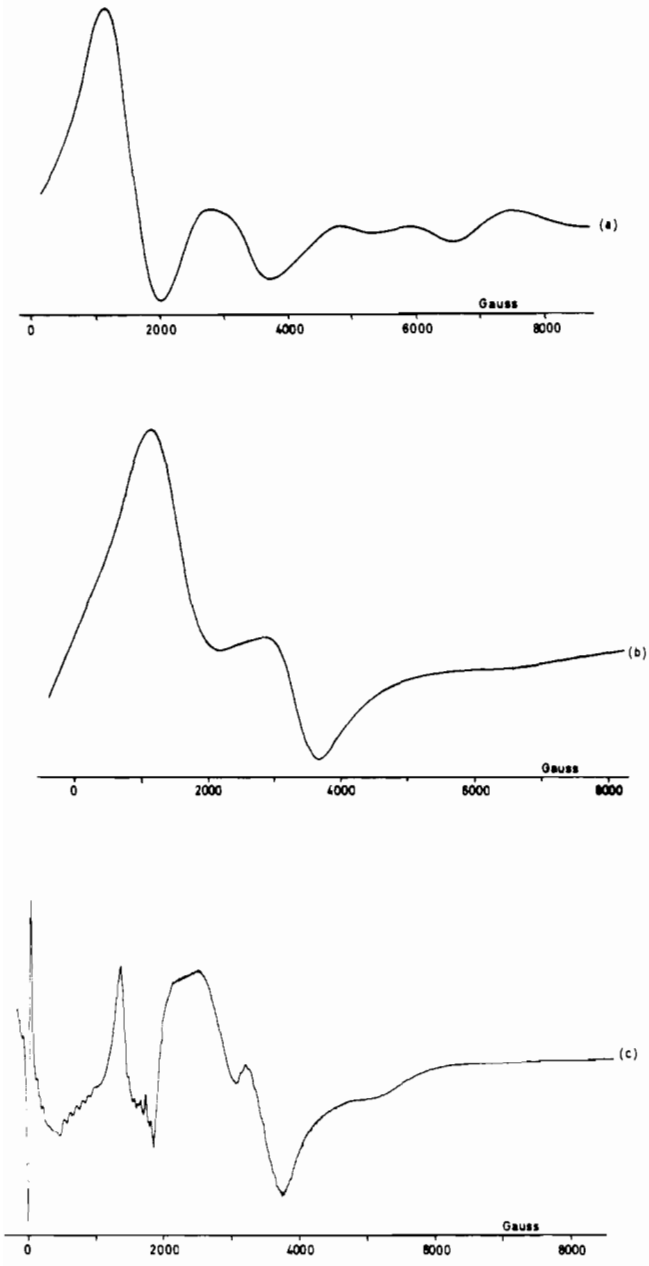

Figure 4. X-Band EPR spectra: (a) complex **4**, Mn^{II}(saldpt)·$2H_2O$, powder at 300 K (microwave power 25 mW, microwave frequency 9.515 GHz, 25-G modulation amplitude); (b) complex **5**, Mn^{II}(5-NO_2-saldpt), powder at 300 K (microwave power 40 mW, microwave frequency 9.414 GHz, 25-G modulation amplitude); (c) complex **5**, DMF/toluene glass at 4.2 K (microwave power 25 mW, microwave frequency 9.436 GHz, 10-G modulation amplitude).

complexes **4** and **5** have near-axial symmetries with λ very close to zero and D values larger than 0.2 cm^{-1} ($\lambda = E/D$; D and E are the axial and rhombic zero-field splitting parameters, respectively).

The complete magnetic susceptibility data for these two complexes[28] afford effective magnetic moments μ_{eff}/Mn relatively independent of temperature except for a small drop at low temperatures. The theoretical approach used for least-squares fitting of the data for a d^5 monomer with axial symmetry has been previously described.[42] Three parameters, $g_\parallel$, $g_\perp$, and the zero-field splitting parameter D were used, and reasonable values were obtained from these fits: Mn^{II}(saldpt)·$2H_2O$ (**4**), $g_\parallel = 2.00$, $g_\perp = 2.00$, $D = 1.41$ cm^{-1}; Mn^{II}(5-NO_2-saldpt)·$2H_2O$ (**5**), $g_\parallel = 2.05$, $g_\perp = 2.05$, $D = 2.17$ cm^{-1}. This, together with the EPR results, confirms that complexes **4** and **5** are monomeric compounds.

X-Band (120 and 4.2 K) and Q-band (120 K) EPR spectra were also obtained for frozen-solution samples of complexes **4** and **5** in a coordinating solvent mixture (DMF/toluene). All these spectra exhibit at least one resonance structured by manganese-55 hyperfine patterns. The X-band spectra are almost identical at both temperatures and characteristic of distorted octahedral symmetries. When the powder and glass spectra are compared, compound **5** shows a change in the coordination geometry, probably due to the coordination of a DMF molecule at the sixth manganese coordination site (Figure 4b,c). On the other hand, complex **4** exhibits almost identical DMF/toluene glass and powder spectra, which is consistent with the coordination of one water molecule in the solid state for this hydrated complex. The Q-band spectra exhibit essentially the $-^1/_2 \rightarrow {}^1/_2$ transition characterized by a strong resonance occurring near $g = 2$. A more detailed description of these spectra, in connection with the examination of the hyperfine patterns, will be given in a subsequent section.

Mn^{II}(saldien) (2). Complex **2**, also characterized by a N_3O_2 ligand donor set, differs from the two previous complexes (**4** and **5**) by the length of the bridging units (ethylene instead of propylene) intervening between the three nitrogen donors. The X-band powder (Figure 5a) and frozen-solution (Figure 5b) spectra are similar, the main difference being that while the powder spectrum exhibits broad fine-structure resonances without any resolved manganese hyperfine pattern, the glass spectrum (Figure 5b) exhibits better resolved fine-structure resonances. Six of these resonances are further split into an 11-line pattern with relative intensities close to the ratios 1:2:3:4:5:6:5:4:3:2:1. The hyperfine coupling constant for these patterns is 40 ± 2 G. The hyperfine intensity pattern and magnitude of constant clearly indicate that in frozen solution this complex is dimeric, $[Mn^{II}(saldien)]_2$. The temperature dependence of these powder and glass EPR spectra is mainly characterized by an intensity decrease and a broadening of the previously described patterns when the temperature is raised from 4.2 to 120 K. The Q-band frozen-solution EPR (Figure 5c) does not afford such a nicely resolved spectrum as the X-band. However fine-structure transitions may be still discerned, four of them being further split into the 11-line pattern previously described.

Coupling two $S = {}^5/_2$ ions gives a system comprised of 36 spin states, which can be grouped into six spin manifolds where $S = 0, 1, 2, 3, 4$, and 5. Each spin manifold has a degeneracy of $2S + 1$ and, as pointed out by several authors,[44,45] may have a different zero-field splitting. There are 30 possible allowed EPR transitions ($\Delta M_S = 1$) for each magnetic field orientation, or 90 in total. There is also the possibility of transitions with $\Delta M_S \neq 1$. Obviously, in the case of even the best behaved spectrum, assignment of these transitions and evaluation of the spin Hamiltonian parameters are difficult. Nevertheless, the number of observed EPR transitions in the spectrum of a pair of Mn^{II} ions may be much greater than the number for a monomeric complex. When compared to the spectra of the monomeric complexes as pictured in Figure 4, the spectrum of $[Mn^{II}(saldien)]_2$ exhibits more fine-structure features that are more closely spaced. This is a first indication of the dimeric nature of complex **2**.

In the case of the hyperfine pattern, Owen[46] showed that if $J \gg A$, the hyperfine interaction of a pair of similar exchange-coupled paramagnetic ions is of the form $(A/2)S\cdot(I_i + I_j)$, which gives rise to a characteristic structure that unambiguously labels the spectrum from a pair. Since $I_i = I_j = {}^5/_2$ for ^{55}Mn, there are 11 lines corresponding to the allowed values of the total nuclear magnetic quantum number $M_I = 5, 4, \ldots, -5$. The expected intensity ratios corresponding to the different ways of building up each M_I value are 1:2:3:4:5:6:5:4:3:2:1. The interline separation for the binuclear complex is $A/2$, that is, half the value found for a monomeric complex. The first example of manganese pairs

(43) (a) Dowsing, R. D.; Gibson, J. F. *J. Chem. Phys.* **1969**, *50*, 294–303. (b) Dowsing, R. D.; Gibson, J. F.; Goodgame, D. M.; Goodgame, M.; Hayward, P. J. *Nature (London)* **1968**, *219*, 1037–1038.

(44) Harris, E. A. *J. Phys. C* **1972**, *5*, 338–352.

(45) McPherson, G. L.; Rong Chang, J. *Inorg. Chem.* **1976**, *15*, 1018–1022.

(46) Owen, J. *J. Appl. Phys.* **1961**, *32*, 213S–217S.

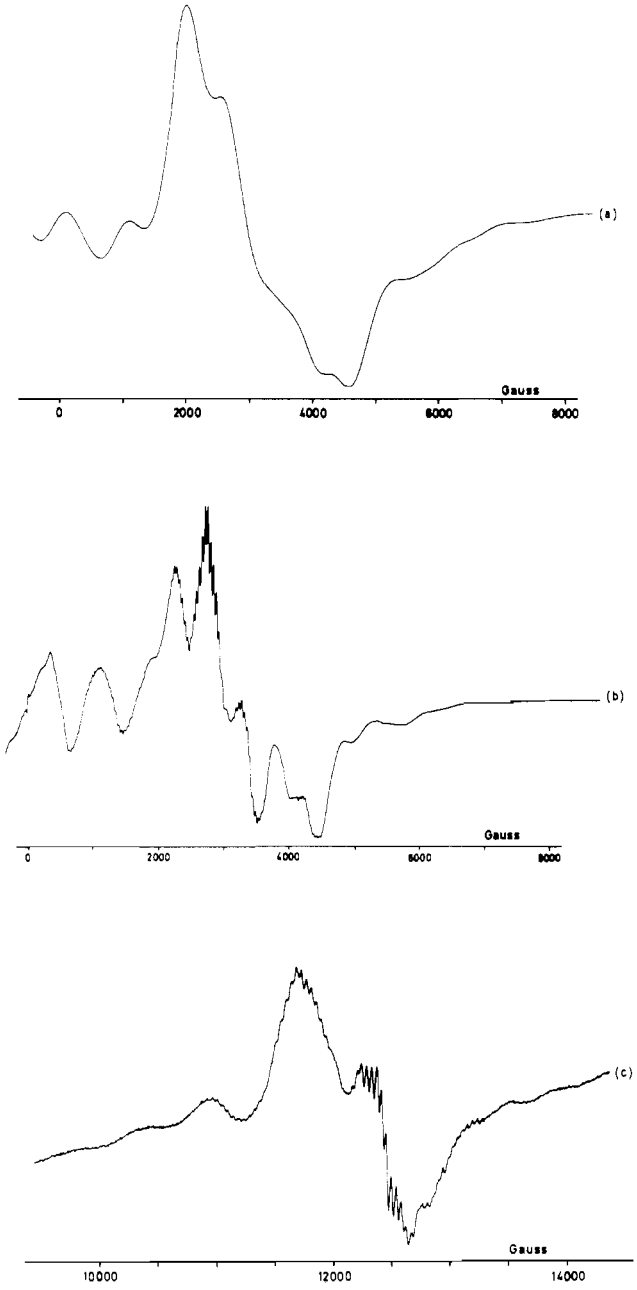

Figure 5. EPR spectra of complex **2**, Mn^{II}(saldien): (a) powder at 4.2 K (microwave power 2 mW, microwave frequency 9.444 GHz, 4-G modulation amplitude); (b) DMF/toluene glass at 4.2 K (microwave power 20 mW, microwave frequency 9.436 GHz, 10-G modulation amplitude); (c) DMF/toluene glass at 120 K (microwave power 2.5 mW, microwave frequency 34.043 GHz, 10-G modulation amplitude).

leading to this characteristic 11-line hyperfine pattern was observed for Mn^{2+}-doped MgO crystals.[47] A few more examples have been described since, including a bis(acetylacetonato)manganese(II) dimer,[48] Mn^{II}-doped $CsCdCl_3$,[45] Mn_2 and Mn_5 molecules in rare-gas matrices,[49] and very recently a binuclear manganese(II) semiquinone complex.[21a] The 11-line pattern superimposed on the six central fine-structure lines of the $[Mn^{II}(saldien)]_2$ spectra (Figure 5), which is characterized by a 40 ± 2 G hyperfine coupling constant and relative intensities close to the expected ratios for a ^{55}Mn pair, unambiguously confirms that this complex is dimeric.

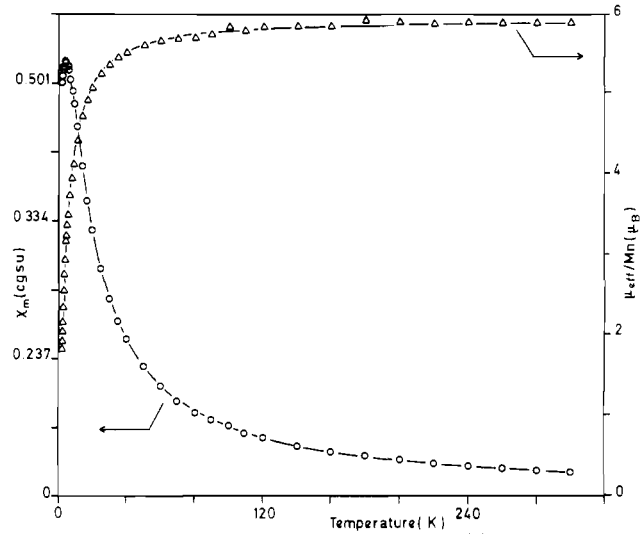

Figure 6. Variable-temperature magnetic susceptibility data for Mn^{II}(saldien). The solid lines result from a least-squares fit of the data to the theoretical equation for isotropic magnetic exchange in a binuclear complex with $S_1 = S_2 = {}^5/_2$.

The magnetic susceptibility data for $[Mn^{II}(saldien)]_2$ have been collected down to 1.7 K.[28] The effective magnetic moment, though relatively constant down to 70 K, exhibits a regular decrease from 5.71 to 1.85 μ_B/Mn between 70 and 1.70 K. These magnetic data can be fitted by using two different methods. In the first model axial single-ion zero-field interactions are included. The theoretical expressions for an exchange-interacting $S_1 = S_2 = {}^5/_2$ dimer, including single-ion zero-field splitting, are detailed elsewhere.[42] An isotropic exchange interaction was assumed as was the presence of axial zero-field splitting (i.e., $D\hat{S}_z^2$). Assuming an isotropic g value of 2.0, the data can be least-squares fit (via matrix-diagonalization techniques) to the dimer equation. Values of $J = -0.63$ cm^{-1} and $D = -810^{-8}$ cm^{-1} are obtained. It should be noted that in this model all spin manifolds have the same amount of zero-field splitting. While the value of J seems reasonable, a D value of ca. -10^{-7} cm^{-1} would appear to be too small to allow a $g = 3.2$ resonance to dominate the X-band powder EPR spectrum (Figure 5a). However, it must be kept in mind that D for a given spin manifold may vary considerably from this value. McPherson[45] has shown D to range from 0.623 cm^{-1} for $S = 1$ to 0.033 cm^{-1} for $S = 5$ for manganese(II) pairs in $CsCdCl_3$. It must also be mentioned that the zero-field splitting in a compound such as Mn^{II}(saldien) is due largely to spin–orbit admixture of excited states into the $^6A_1$ single-ion ground state with a very minor contribution from low-symmetry crystal fields. The zero-field splitting is a single-ion property even for such a dimer, because with the very appreciable metal–metal distances the interion dipolar zero-field splitting is negligible. Considering the very small "average" value of D resulting from the previous fit, the data were also least-squares fit in the second model to the theoretical equation[50] for an isotropic magnetic exchange interaction between two $S_1 = S_2 = {}^5/_2$ ions by employing the simpler $\hat{H} = -2JS_1 \cdot S_2$ spin Hamiltonian. The lines in Figure 6 represent this fit, which can be seen to be good. Least-squares fitting parameters are $J = -0.65$ cm^{-1} and $g_{av} = 2.00$. It is gratifying to see that these values are in close agreement with the previous ones. Finally, the magnetic susceptibility results confirm again that the Mn^{II}(saldien) complex has to be formulated as a dimer. The two manganese(II) ions are antiferromagnetically coupled with a small J value, which indicates either a quite large Mn–Mn distance or an ineffective orbital-exchange pathway.

On the basis of IR and electrochemistry results, Taylor et al.[22d] suggested for the Mn^{II}(saldien) complex a dimeric formulation similar to that of Cu^{II}(saldien).[51] Such a centrosymmetric dimer

(47) Coles, B. A.; Orton, J. W.; Owen, J. *Phys. Rev. Lett.* **1960**, *4*, 116–117.
(48) Hudson, A.; Kennedy, M. J. d. G. *Inorg. Nucl. Chem. Lett.* **1971**, *7*, 333–336.
(49) (a) Van Zee, R. J.; Baumann, C. A.; Weltner, W., Jr. *J. Chem. Phys.* **1981**, *74*, 6977–6978. (b) Baumann, C. A.; Van Zee, R. J.; Bhat, S. V.; Weltner, W., Jr. *J. Chem. Phys.* **1983**, *78*, 190–199.
(50) Spiro, C. L.; Lambert, S. L.; Smith, T. J. Duesler, E. N.; Gagne, R. R.; Hendrickson, D. N. *Inorg. Chem.* **1981**, *20*, 1229–1237.

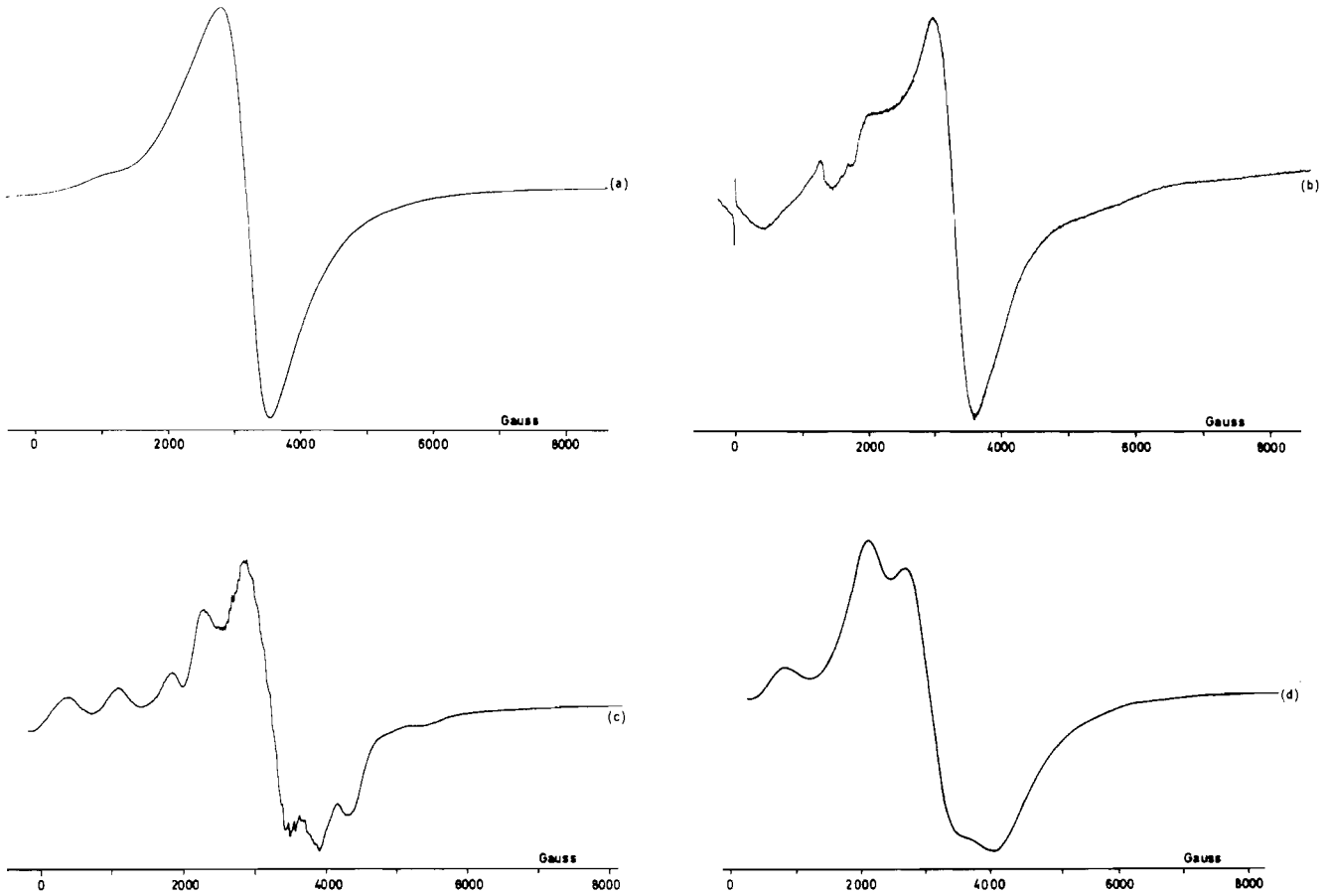

Figure 7. X-Band EPR spectra of complex **3**, $Mn^{II}(5\text{-}NO_2\text{-saldien})\cdot CH_3OH$: (a) powder at 300 K (microwave power 25 mW, microwave frequency 9.412 GHz, 25-G modulation amplitude); (b) DMF/toluene glass at 120 K (microwave power 40 mW, microwave frequency 9.410 GHz, 10-G modulation amplitude); (c) $C_2H_4Cl_2$ frozen solution at 120 K (microwave power 25 mW, microwave frequency 9.408 GHz, 10-G modulation amplitude); (d) powder at 300 K resulting from the evaporation of a $C_2H_4Cl_2$ solution of complex **3** (microwave power 10 mW, microwave frequency 9.418 GHz, 10-G modulation amplitude).

where each ion is pentacoordinated with three donor atoms from one saldien ligand and two from the other saldien ligand is attractive because it would result in a quite large manganese–manganese distance with two N–C–C–N bridging units between the two metal ions. However, we have found from a comparison of X-ray diffraction powder patterns[52] that $[Mn^{II}(saldien)]_2$ is not isostructural with $[Cu^{II}(saldien)]_2$. By a slightly different synthetic route than that described in the Experimental Section, crystals of $Mn^{II}(saldien)\cdot H_2O$ were obtained from a methanol/ethanol/water mixture. When dissolved in a DMF/toluene mixture, these crystals afford the same EPR spectra as those obtained from a methanol/ethanol mixture, confirming the dimeric nature of the hydrate. Owing to the poor quality of the crystals, the full structure determination was not possible. However, the monoclinic unit cell dimensions were obtained as a = 12.30 (2) Å, b = 15.61 (2) Å, c = 19.54 (3) Å, and β = 108.2 (1)°. The results obtained by McKenzie and Selvey[51] for Cu^{II}(saldien) are a = 12.86 (1) Å, b = 16.74 (2) Å, c = 9.86 (1) Å and β = 105.1 (1)° for a monoclinic unit cell.

In another attempt to draw a comparison between these two complexes we measured the magnetic susceptibility of $[Cu^{II}(saldien)]_2$ between 300 and 1.7 K. The results[28] indicate that there is no detectable interaction between the two copper ions. In contrast, it is interesting to note that for Fe^{II}(saldien), J.-P.T. and D.N.H.[53] were able to observe an antiferromagnetic interactions of the same order of magnitude ($J = -2.2$ cm^{-1}) between the two ferrous ions, as we found for $[Mn^{II}(saldien)]_2$. Thus, it may be suggested that among these three dimeric saldien complexes the ferrous and the manganous ones may have similar solid-state structures while the cupric complex must have a different one. In this respect, the structure proposed by Zelentsov et al.,[54] which involves a bridged

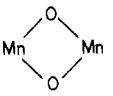

fragment including two phenolic oxygen atoms for parent Mn(II) and Mn(III) Schiff base complexes, may be an attractive structural hypothesis for the ferrous and manganous saldien complexes (Figure 3b).

$Mn^{II}(5\text{-}NO_2\text{-saldien})\cdot CH_3OH$ (3). Complex **3**, although having the same donor set and ethylene bridging units as $[Mn^{II}(saldien)]_2$, exhibits a quite different magnetic behavior from that of complex **2**. Figure 7 exemplifies a few EPR spectra afforded by $Mn^{II}(5\text{-}NO_2\text{-saldien})$ with different experimental conditions. The X-band powder spectrum (Figure 7a) is almost temperature-independent and characterized by a broad $g \approx 2$ main resonance with a small $g \approx 6$ shoulder. Owing to the fact that three nitrogen atoms are involved in the coordination sphere of the manganese(II) (cf. IR

(51) McKenzie, E. D.; Selvey, S. J. *Inorg. Chim. Acta* **1976**, *18*, L1–L2.
(52) The X-ray diffraction powder patterns were obtained with a Guinier powder diffractograph (Cu Kα wavelength). The $Mn^{II}(5\text{-}NO_2\text{-saldien})\cdot CH_3OH$ complex, which exhibits no diffraction pattern, seems to be an amorphous material. A comparison of the reflections observed for Cu^{II}(saldien) and Mn^{II}(saldien) powder samples shows several differences between the two patterns. This comparison allows us to conclude that even though they may have a few comparable crystallographic parameters, these two complexes do not present identical unit cells.
(53) Tuchagues, J.-P.; Hendrickson, D. N. *Inorg. Chem.* **1983**, *22*, 2545–2552.
(54) (a) Zelentsov, V. V.; Somova, I. K.; Kurtanidze, R. Sh.; Nikolaeva, T. B. *Koord. Khim.* **1980**, *6*, 1576–1579. (b) Zelentsov, V. V.; Somova, I. K.; Kurtanidze, R. Sh.; Korotkova, V. V.; Tsintsadze, G. V. *Koord. Khim.* **1981**, *7*, 1072–1080.

Table VI. Selected IR and EPR Observations Evidencing the Presence of Isomers for Complexes **4**–**13**

	KBr pellet IR no. of frequencies obsd		DMF/toluene glass EPR								
			X-band (4.2 K)			Q-band (120 K)					
complex	NH str	CH_2 rock	no. of hyperfine patterns obsd	A, G	av field, G	g	A, G	g_{cis}	A_{cis}, G	g_{trans}	A_{trans}, G
4	2	5	2	94, 91	1700	2.009	91				
5	1	2	1	88	1775	1.980	89				
6		2	2	94, 94	1663			1.987	88	1.984	88
7		4	2	94, 90	1650			2.008	87	1.996	87
8	2	6						2.058	86	2.000	86
9	2	6	1	88	1200			2.057	88	1.997	89
10	1 (vs, broad)	6	2	96, 83	1675	2.001	91				
11	2	6	2	overlapping	1600			2.011	89	1.980	84
12	2	6	2	91, 88	1700			2.005	90	1.980	88
13	1 (vs, broad)	6	2	overlapping	1580			2.008	91	1.980	88

section), this complex would be expected to afford an axial type EPR spectrum. However, the presence of methanol in the formula of the complex may lead to the situation where the methanolic oxygen is acting as a sixth ligand atom. This interpretation seems to be confirmed by the frozen-solution spectrum obtained with a coordinating DMF/toluene solvent mixture (Figure 7b), which is also characteristic of a distorted octahedral symmetry. More surprising is the EPR spectrum obtained from a $C_2H_4Cl_2$ frozen solution. With such a noncoordinating solvent the EPR spectrum of Mn^{II}(5-NO_2-saldien), even though poorly resolved, is very similar to that afforded by Mn^{II}(saldien), i.e. a dimer type spectrum with the characteristic 11-line hyperfine pattern resolved on three of the fine-structure resonances (Figure 7c).

In order to understand better the behavior of this complex, which seems to be dramatically influenced by the presence of methanol in the solid state, we tried to take out the methanol. (i) When heating under vacuum a powder sample of the complex Mn^{II}(5-NO_2-saldien)·CH_3OH for 2–16 h at a temperature ranging from 80 to 160 °C, we were unable to take more than 10–20% of the methanol out of the sample according to the analytical results. The EPR spectra obtained from the samples heated under vacuum were identical with those of the starting material. (ii) A powder sample of Mn^{II}(5-NO_2-saldien)·CH_3OH was dissolved in $C_2H_4Cl_2$ in the drybox. The resulting solution was evaporated under vacuum to afford a yellow-orange powder. The powder EPR spectrum of the resulting sample gave the trace spectrum of Figure 7d, which is dramatically different from the powder EPR of the starting material (Figure 7a) and is indicative of a dimer type structure. Two conclusions may be drawn from these experiments: The methanol present in the complex Mn^{II}(5-NO_2-saldien)·CH_3OH is tightly bound to the manganese, probably as a sixth ligand. The $C_2H_4Cl_2$ frozen-solution spectrum (Figure 7c) of complex **3** and the powder spectrum (Figure 7d) of the recrystallized sample obtained as described in (ii) are similar and indicative of a dimeric structure. This implies removal of methanol in both cases, which results in the destruction of association between hexacoordinated solvated species.

The effective magnetic moment per manganese for complex **3**[28] though relatively constant down to 100 K exhibits a regular decrease from 5.72 μ_B at 100 K to 4.49 μ_B at 4.7 K. This behavior is characteristic of solid-state magnetic interactions between manganese ions. We were unable to obtain a good fit of the experimental data of complex **3** when using the previously mentioned theoretical expressions for an exchange-interacting $S_1 = S_2 = {}^5/_2$ dimer, with or without zero-field splitting. This result may be understood as due to the fact that the bound methanol molecule not only provides a sixth ligand atom for the manganese ion but at the same time allows weak intermolecular manganese interactions.

Mn^{II}(salprenOH) (1). Although involving a potentially pentadentate ligand as with the four previous complexes, compound **1** is characterized by a N_2O_3 ligand donor set instead of the N_3O_2 one. The X-band spectra of either powdered samples or frozen glasses are almost identical between 4 and 300 K. These spectra are characterized by a very broad $g \approx 2$ centered resonance without manganese hyperfine structure. Dowsing et al.[41a,43b] observed similar very broad $g \approx 2$ centered resonances for the complexes $Mn^{II}(\gamma\text{-picoline})_2X_2$. They explained these observations as resulting from polymer-like structure affording extended intermolecular magnetic interactions.

The effective magnetic moment per manganese for complex **1**[28] slowly decreases from 6.04 μ_B at 300 K to 3.51 μ_B at 4.3 K. From the earlier mentioned theoretical expressions for an exchange-coupled dimer, a reasonable fit may be obtained.[28] However, assuming no zero-field splitting, this fit involved a quite low average g value of 1.8, with $J = -3.3$ cm^{-1}. In order to give a better account for both the variable-temperature magnetic susceptibility data and the EPR results, we need to consider extended intermolecular interactions. J.-P.T. and D.N.H. recently reported similar magnetic susceptibility results[53] for the parent complex Fe^{II}(salprenOH). The decrease in the Fe^{II} effective magnetic moment observed (from 5.36 μ_B at 300 K to 3.56 μ_B at 4.2 K) was attributed to intermolecular interactions mediated by the secondary alcoholic function of the ligand.

Complexes with N_4O_2 Ligand Donor Sets (6–13). Complexes **6** and **7**, Mn^{II}(salaep)$_2$·$2H_2O$ and Mn^{II}(5-NO_2-salaep)$_2$, each have two tridentate ligands characterized by a N_2O donor set. Complexes **8**–**13** of general formulation Mn^{II}[Zsal-N(a,b,c,d)] incorporate a hexadentate ligand characterized by a N_4O_2 donor set.

The EPR spectra of powder samples of complexes **6**–**9**, **12**, and **13**, recorded at 4.2, 120, and 300 K, do not show appreciable temperature dependence. The resonances are broad, and the manganese hyperfine splitting is not resolved. Complexes **8** and **12**[28] exhibit an isotropic $g \approx 2$ resonance, consistent with an almost pure octahedral symmetry.[41a,43] The spectrum of complex **7**[28] shows five fine-structure transitions, indicative of a slightly distorted octahedral symmetry with low D and E values (0.001–0.1 cm^{-1}) and λ different from ${}^1/_3$.[41a,43] The spectrum of complex **6**[28] shows additional low- and high-field transitions, which are indicative of higher D and E values due to either a more distorted octahedral geometry or the intervention of two different types of ligands (coordinated solvent for example). The spectra of complexes **9** and **13**[28] exhibit a main resonance near $g = 4.3$, indicating a distorted octahedral symmetry with D and $E < 0.1$ cm^{-1} and $\lambda \approx {}^1/_3$. As is shown below, this distortion has been confirmed by the X-ray structure determination of complex **13**. The spectra of complexes **10** and **11**[28] exhibit, in addition to the main resonance near $g = 4.3$, several lines at low field and high field, one of which is at lower field than 650 G. According to Dowsing et al.[43a] and Griffith,[55] this indicates D values approximately equal to $h\nu$ and

(55) Griffith, J. S. *Mol. Phys.* **1964**, *8*, 213–216.
(56) Hughes, B. B.; Haltiwanger, R. C.; Pierpont, C. G.; Hampton, M.; Blackmer, G. L. *Inorg. Chem.* **1980**, *19*, 1801–1803.
(57) Stephens, F. S. *Acta Crystallogr., Sect. B: Struct. Crystallogr. Cryst. Chem.* **1977**, *B33*, 3492–3496.
(58) Avdeef, A.; Costamagna, J. A.; Fackler, J. P. *Inorg. Chem.* **1974**, *13*, 1854–1863.
(59) Mikuriya, M.; Torihara, N.; Okawa, H.; Kida, S. *Bull. Chem. Soc. Jpn.* **1981**, *54*, 1063–1067.
(60) Stein, J.; Fackler, J. P.; McLure, G. J.; Tee, J. A.; Chan. L. T. *Inorg. Chem.* **1979**, *18*, 3511–3519.

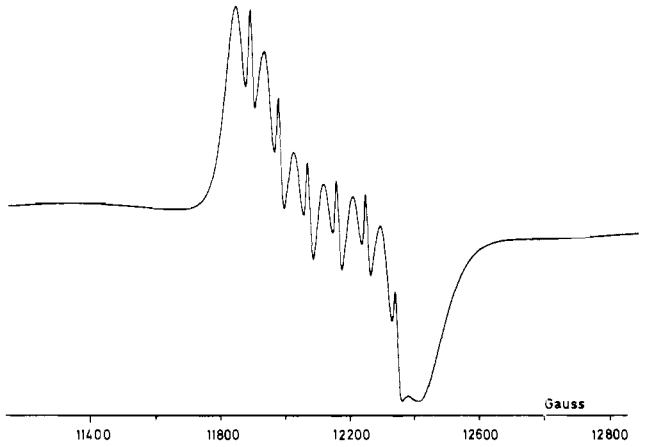

Figure 8. Q-Band DMF/toluene glass spectrum of complex **7**, Mn^{II}(5-NO_2-salaep)$_2$, at 120 K (microwave power 2.7 mW, microwave frequency 33.971 GHz, 10-G modulation amplitude).

λ values close to $^1/_3$. It is interesting to note that the kind of spectrum exhibited by complexes **10** and **11** together with the resulting E and D values was predicted by these authors for distorted octahedral complexes having in-plane donor atoms forming a rectangle rather than a square. This prediction is perfectly consistent with the observation of such a distorted symmetry for the two complexes having the three consecutive bridging units $(CH_2)_3$, $(CH_2)_2$, and $(CH_2)_3$ between the four nitrogen donors.

The previous EPR observations are in overall agreement with a monomeric formulation of complexes **6–13**. Most of these complexes have zero-field splitting terms different from zero, which indicates that they have symmetries that depart more or less from the regular cubic one expected for pure octahedral geometry.

The room-temperature solution spectra of the N_4O_2 ligand complexes dissolved in DMF/toluene and $C_2H_4Cl_2$/toluene mixtures exhibit broad, weak, $g \approx 2$ centered resonances. The frozen-solution spectra in $C_2H_4Cl_2$/toluene glasses are nearly identical with the corresponding powder spectra. In particular, no manganese hyperfine structure is observed.

On the other hand, the spectra obtained from DMF/toluene glasses at 120 and 4.2 K are very different from the powder, solution, and $C_2H_4Cl_2$/toluene glass spectra for the N_4O_2 ligand complexes. These spectra are comprised of different, more numerous, and better resolved fine-structure resonances. Manganese hyperfine structure is observed for most complexes on several fine-structure resonances and is anisotropic.[28] This is probably due to the fact that in DMF the coordination geometry around the manganese(II) ion is slightly modified. Moreover, all complexes **6–13** show a zero-field transition, which in most cases is split by the coupling of the electron spin with the manganese-55 nuclear spin.[28] These zero-field transitions give evidence for the departure from the octahedral symmetry expected for such hexacoordinated complexes when dissolved in DMF/toluene mixtures.

DMF/toluene frozen-solution spectra were also recorded at Q-band for complexes **6–13** at 120 K. As expected, most of them exhibit essentially the $g \approx 2$ resonance split by manganese hyperfine structure. As exemplified in Figure 8, the spectra consist of two superimposed but slightly shifted six-line patterns. Similar patterns were observed in the X-band DMF/toluene glass spectra for complexes **6**, **7**, and **10–13** as well as for the pentacoordinated complex **4** previously discussed. The separation between the two manganese six-line patterns is larger at Q-band than at X-band.

Table VII. Bond Lengths (Å) and Bond Angles (deg) for Mn^{II}[5-NO_2-sal-N(1,5,9,13)]·0.65$C_2H_4Cl_2$ with Estimated Standard Deviations in Parentheses

		Mn Environment	
Mn–O(1)	2.110 (4)	Mn–N(2)	2.291 (5)
Mn–O(2)	2.173 (4)	Mn–N(3)	2.380 (4)
Mn–N(1)	2.273 (4)	Mn–N(4)	2.269 (5)
O(1)–Mn–O(2)	158.1 (2)	O(2)–Mn–N(4)	79.2 (2)
O(1)–Mn–N(1)	81.6 (1)	N(1)–Mn–N(2)	82.3 (2)
O(1)–Mn–N(2)	110.2 (2)	N(1)–Mn–N(3)	157.9 (2)
O(1)–Mn–N(3)	84.6 (1)	N(1)–Mn–N(4)	110.4 (2)
O(1)–Mn–N(4)	85.3 (2)	N(2)–Mn–N(3)	86.5 (2)
O(2)–Mn–N(1)	89.4 (1)	N(2)–Mn–N(4)	161.6 (2)
O(2)–Mn–N(2)	88.1 (2)	N(3)–Mn–N(4)	85.4 (2)
O(2)–Mn–N(3)	109.2 (1)		
		Ligand Environment	
O(1)–C(1)	1.294 (6)	O(2)–C(15)	1.285 (7)
C(1)–C(2)	1.449 (8)	C(15)–C(14)	1.452 (9)
C(2)–C(3)	1.465 (8)	C(14)–C(13)	1.459 (8)
C(3)–N(1)	1.285 (7)	C(13)–N(4)	1.265 (7)
N(1)–C(4)	1.470 (7)	N(4)–C(12)	1.471 (7)
C(4)–C(5)	1.519 (9)	C(12)–C(11)	1.534 (9)
C(5)–C(6)	1.505 (8)	C(11)–C(10)	1.523 (9)
C(6)–N(2)	1.501 (7)	C(10)–N(3)	1.468 (7)
N(2)–C(7)	1.485 (7)	N(3)–C(9)	1.479 (8)
C(7)–C(8)	1.530 (9)	C(9)–C(8)	1.515 (8)
C(1)–C(19)	1.417 (8)	C(14)–C(23)	1.385 (9)
C(19)–C(18)	1.371 (8)	C(23)–C(22)	1.372 (9)
C(18)–C(17)	1.380 (8)	C(22)–C(21)	1.408 (10)
C(17)–C(16)	1.393 (8)	C(21)–C(20)	1.331 (9)
C(16)–C(2)	1.370 (7)	C(20)–C(15)	1.438 (8)
C(17)–N(5)	1.454 (7)	C(22)–N(6)	1.434 (10)
N(5)–O(3)	1.241 (8)	N(6)–O(5)	1.206 (10)
N(5)–O(4)	1.240 (9)	N(6)–O(6)	1.226 (9)
Mn–O(1)–C(1)	132.2 (3)	Mn–O(2)–C(15)	122.5 (3)
O(1)–C(1)–C(2)	123.6 (5)	O(2)–C(15)–C(14)	123.5 (5)
C(1)–C(2)–C(3)	122.3 (5)	C(15)–C(14)–C(13)	121.7 (5)
C(2)–C(3)–N(1)	126.9 (5)	C(14)–C(13)–N(4)	125.9 (5)
Mn–N(1)–C(3)	126.7 (4)	Mn–N(4)–C(13)	123.1 (4)
Mn–N(1)–C(4)	118.1 (3)	Mn–N(4)–C(12)	118.6 (3)
C(3)–N(1)–C(4)	115.1 (5)	C(13)–N(4)–C(12)	117.6 (5)
N(1)–C(4)–C(5)	111.4 (4)	N(4)–C(12)–C(11)	111.1 (5)
C(4)–C(5)–C(6)	114.8 (5)	C(12)–C(11)–C(10)	113.9 (5)
C(5)–C(6)–N(2)	112.9 (5)	C(11)–C(10)–N(3)	113.8 (5)
Mn–N(2)–C(6)	114.5 (3)	Mn–N(3)–C(10)	114.9 (3)
Mn–N(2)–C(7)	108.3 (3)	Mn–N(3)–C(9)	103.8 (3)
C(6)–N(2)–C(7)	111.1 (4)	C(10)–N(3)–C(9)	109.1 (4)
N(2)–C(7)–C(8)	112.5 (5)	N(3)–C(9)–C(8)	116.1 (5)
C(7)–C(8)–C(9)	113.4 (5)		
O(1)–C(1)–C(19)	120.2 (5)	O(2)–C(15)–C(20)	120.4 (5)
C(3)–C(2)–C(16)	116.9 (5)	C(13)–C(14)–C(23)	118.6 (5)
C(2)–C(1)–C(19)	116.2 (5)	C(15)–C(14)–C(23)	119.2 (5)
C(1)–C(2)–C(16)	120.4 (5)	C(14)–C(15)–C(20)	116.1 (5)
C(2)–C(16)–C(17)	120.0 (5)	C(15)–C(20)–C(21)	123.1 (6)
C(16)–C(17)–C(18)	121.5 (5)	C(20)–C(21)–C(22)	119.6 (6)
C(17)–C(18)–C(19)	119.0 (5)	C(21)–C(22)–C(23)	120.4 (6)
C(18)–C(19)–C(1)	122.6 (6)	C(22)–C(23)–C(14)	121.5 (6)
C(16)–C(17)–N(5)	117.4 (5)	C(21)–C(22)–N(6)	121.9 (6)
C(18)–C(17)–N(5)	121.0 (5)	C(23)–C(22)–N(6)	117.6 (6)
C(17)–N(5)–O(3)	116.7 (6)	C(22)–N(6)–O(5)	121.4 (7)
C(17)–N(5)–O(4)	119.9 (5)	C(22)–N(6)–O(6)	115.6 (7)
O(3)–N(5)–O(4)	123.4 (5)	O(5)–N(6)–O(6)	122.9 (7)

The observation of the splitting of the NH and CH_2 stretching frequencies as well as the CH_2 rocking frequencies in the IR spectra of these same complexes in the solid state together with the observation of the splitting of the manganese hyperfine structure in the frozen DMF/toluene glass EPR spectra is indicative of simultaneous NH, CH_2, and Mn inequivalences. These simultaneous inequivalences lead us to conclude that two different isomers of these complexes are present both in the solid state and in solution.

The overall results concerning the IR and EPR observations related to these splittings have been collected in Table VI. As shown in Figure 9 for the hexacoordinated complexes there are

(61) Stults, B. R.; Marianelli, R. S.; Day, V. W. *Inorg. Chem.* **1975**, *14*, 722–730.
(62) Plaskin, P. M.; Stoufer, R. C.; Mathew, M.; Palenik, G. J. *J. Am. Chem. Soc.* **1972**, *94*, 2121–2122.
(63) Hartman, J. R.; Foxman, B. M.; Cooper, S. R. *J. Chem. Soc., Chem. Commun.* **1982**, 583–584.
(64) Camenzind, M. J.; Hollander, F. J.; Hill, C. L. *Inorg. Chem.* **1982**, *21*, 4301–4308.

Table VIII. Representative Mn–O and Mn–N Bond Lengths in Mn(II), Mn(III), and Mn(IV) Complexes

complex	Mn oxidn state	Mn–O, Å	Mn–N, Å	ref
Mn[5-NO_2-sal-N(1,5,9,13)]	II	2.110 (4)–2.173 (4)	2.269 (5)–2.380 (4)	this work
$Mn_2(tren)_2(NCS)_2^{2+}$	II		2.100 (4)–2.343 (3)	43
$Mn_4(3,5\text{-DBSQ})_8$	II	2.062 (5)–2.526 (7)		19
$Mn(12\text{-crown-4})_2^{2+}$	II	2.24 (2)–2.37 (2)		56
$Mn(acac)_2(phen)$	II	2.116 (5)–2.152 (5)	2.307 (5)	57
$Mn(trop)_3$	III	2.001		58
Mn(spa)(ac)	III	1.849 (2)–1.951 (2)	2.006 (2)	59
$Mn(EDTA)^-$	III	1.898 (11)–2.036 (12)	2.223 (14)	60
$[Mn(acac)_2(N_3)]_n$	III	1.910 (1)	2.245 (2)	61
$[(bpy)_2MnO]_2^{3+}$	III	1.853–1.856	2.129–2.226	62
$[(bpy)_2MnO]_2^{3+}$	IV	1.784	2.016–2.075	62
$Mn(3,5\text{-DBCat})_2(py)_2$	IV	1.854 (2)	2.018 (3)	19
$Mn(3,5\text{-DBCat})_3^{2-}$	IV	1.891 (3)–1.922 (3)		63
$Mn(TPP)(OCH_3)_2$	IV	1.839 (2)	1.993 (3)–2.031 (3)	64
Mn[sal-N(1,4,7,10)]$(ClO_4)_2$	IV	1.816 (4)	1.964 (4)–2.030 (4)	23

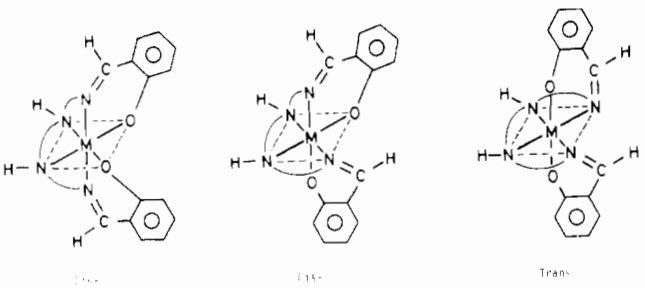

Figure 9. Schematization of the three possible isomers for a hexacoordinated manganese(II) complex with a N_4O_2 donor set.

three possible isomers for each complex. With reference to the phenolic oxygen atoms of the ligands, these isomers can be identified as the cis-α, cis-β, and trans isomers. Likewise, in the pentacoordinated complexes, two cis isomers and one trans isomer may be drawn. Differences in the electronic environments of CH_2, NH, and Mn exist among all three isomers. However, the electronic structure modification around the manganese afforded by the difference between the cis-α and the cis-β coordination spheres must be small compared to the electronic modification afforded around the manganese ion by the difference between the trans and either of the cis isomers. Therefore, we can expect that the EPR will distinguish more readily between the trans isomer and the cis isomers than between the cis-α and the cis-β isomers. The Q-band spectrum shown in Figure 8 does verify this prediction: one of the six-line patterns is characterized by broad resonances and an overall spin density larger than that attributable to the sharp resonances forming the second six-line pattern. It is therefore possible to assign the broad six-line pattern to both cis isomers and the six sharp resonances to the trans isomer.

The effective magnetic moments, μ_{eff}/Mn, for complexes **6–13**[28] are relatively constant except for a small drop (5–10%) below 20–30 K. The theoretical approach previously used for least-squares fitting of the data for a high-spin d^5 monomer with axial symmetry[42] was also used for these complexes. $g_\parallel$ and $g_\perp$ values near 2.0 and D values between 0.4 and 6.0 cm^{-1} afforded quite reasonable fits.[28] However, in light of the powder EPR results, the theoretical D values necessary to fit the magnetic susceptibility data seem too large for some of these complexes. It is perhaps unreasonable to assume that $E = 0$ for most of these complexes. It would seem more consistent to fit these data for a high-spin d^5 monomer with distorted octahedral symmetry by using the g_x, g_y, g_z, D, and E parameters. However, the results already obtained are in overall agreement with the EPR data in the sense that they confirm the monomeric nature of the complexes and quite large distortions of the regular octahedral symmetry for most of these eight complexes. This interpretation is further confirmed in the case of complex **13**, for which a full structure determination has been carried out.

Structural Features of Mn^{II}[5-NO_2-sal-N(1,5,9,13)] (13). The crystal structure of complex **13** has been determined on a crystal of the Mn^{II}[5-NO_2-sal-N(1,5,9,13)]·0.65$C_2H_4Cl_2$ solvate. An ORTEP view of the complex molecule is shown in Figure 2. Bond lengths and bond angles are given in Table VII. As predicted from EPR results, the MnO_2N_4 coordination polyhedron in complex **13** resembles a quite distorted octahedron. This can be seen from the values of the bond angles around the manganese atom listed in Table VII and from the deviations of the manganese atom and the coordinated oxygen and nitrogen atoms from a least-squares plane;[28] all of these deviations are larger than 0.2 Å.

The Mn–O bond lengths of 2.110 (4) and 2.173 (4) Å in complex **13** compare well with the values reported for d^5 Mn(II) complexes that are gathered in Table VIII. In turn, they differ significantly from the values reported for Mn(III) and Mn(IV) complexes. Likewise, the Mn–N bond lengths in complex **13** compare well with the values reported for Mn(II) complexes such as $[Mn_2(tren)_2(NCS)_2]^{2+}$[42] and $Mn(acac)_2(phen)$[57] but are larger than the values reported for Mn(III) and Mn(IV) complexes (Table VIII).

Referring to the possible existence of isomers in the cases of complexes **4–13** discussed earlier, it is interesting to note that in complex **13** both coordinated phenolic oxygen atoms are in a trans configuration while in the related Mn^{IV}[sal-N(1,4,7,10)]$(ClO_4)_2$ complex they are in a cis configuration.[23] Even though a rearrangement of the hexacoordinated ligand is possible on going from the manganese(II) to the manganese(IV) complexes, this observation gives further support to the hypothesis of the presence of isomeric forms in such complexes.

Finally, the intermolecular interatomic distances show no close intermolecular contacts and clearly confirm the monomeric nature of complex **13**: the shortest Mn···Mn distance is 5.814 (2) Å. Only very weak intermolecular hydrogen-bonding contacts have been observed.[28]

In conclusion, the main features of the crystal structure of complex **13**, i.e. monomeric nature and distortion from regular octahedral symmetry, are in agreement with the EPR and magnetic susceptibility results, which indicate the presence of quite large zero-field splitting parameters.

Summary and Comments

The infrared data, chemical analysis, variable-temperature magnetic susceptibility results, and EPR spectra provide evidence that the manganese(II) complexes described in this study are high-spin penta- or hexacoordinated species. The study of the magnetic properties of these 13 complexes indicates that minor changes in the design of polydentate ligands in this same Schiff-base family can lead to either monomeric or dimeric complexes or complexes with extended intermolecular interaction. It is clear that the EPR technique is very sensitive to these changes.

Complex **1**, with its N_2O_3 donor set ligand and alcoholic function between the two imine nitrogen donors, is an example of a structure exhibiting extended intermolecular magnetic exchange interactions.

Complex **2**, with a N_3O_2 donor set ligand with ethylene bridges between the three nitrogen donors, is a dimer as indicated by the

presence of a magnetic exchange interaction. It can be prepared either with or without one water molecule per manganese ion depending on the synthetic route, the sixth coordination site of each manganese ion in the dimer being sterically and electronically accessible to small ligand molecules. It should be noted in this respect that the oxygen oxidation of this dimer has been shown to afford a mixed-valence Mn(II)–Mn(III) complex[24] that exhibits magnetic properties related to those of the oxygen-evolving metalloprotein of photosystem II. Mn^{II}(5-NO_2-saldien)·CH_3OH (**3**) presents extended intermolecular magnetic exchange interactions in the solid state. When dissolved in noncoordinating solvents, it exhibits dimeric properties similar to those of Mn^{II}(saldien).

By lengthening the bridging units between the three nitrogen donors of these pentadentate ligands from ethylene to propylene units and thus giving some more flexibility to the pentadentate ligand, it is possible to obtain monomeric pentacoordinated manganese(II) complexes (compounds **4** and **5**).

Complexes **6** and **7**, characterized by two N_2O donor sets, and complexes **8**–**13**, characterized by a N_4O_2 donor set, have been shown to be monomeric hexacoordinated species with departures from the regular octahedral symmetry more or less marked depending on steric and/or electronic factors. These conclusions have been confirmed by an X-ray molecular structure determination for one of these complexes, Mn^{II}[5-NO_2-sal-N(1,5,9,13)].

Among the complexes studied herein the monomeric compounds **4**–**13** exhibit splitting of the NH and CH_2 stretches and of the CH_2 rocking frequencies in the solid state. They also exhibit a splitting of the manganese hyperfine EPR resonances at both X-band and Q-band when examined as frozen solutions. These observations, indicative of simultaneous NH, CH_2, and Mn inequivalences both in the solid state and in solution, indicate that these complexes may exist in different isomeric forms. Indeed, structural determinations indicate that the Mn^{II}[5-NO_2-sal-N-(1,5,9,13)] crystal is built from trans isomers (this work) while the Mn^{IV}[sal-N(1,4,7,10)]$(ClO_4)_2$ crystal[23] is made from cis-α isomers.

Acknowledgment. We thank the National Institutes of Health for partial support of the work at the University of Illinois through Grant HL 13652 to D.N.H. J.-P.T. and D.N.H. are thankful for a NATO grant for collaborative research. The crystal structure of complex **13** was determined by F. Dahan. Her excellent contribution to this work is gratefully acknowledged. J.-M. Savariault is to be thanked for help in obtaining the X-ray diffraction powder patterns and unit cell dimensions of complex **2**. M. D. Timken and Y. T. Hwang are acknowledged for help in fitting the magnetic susceptibility data.

Registry No. **1**, 69879-57-8; **2**, 101056-15-9; **3**, 101056-16-0; **3**·CH_3OH, 101247-86-3; **4**·H_2O-*trans*, 101224-27-5; **4**·OH_2-*cis*, 101398-95-2; **5**-*trans*, 101056-17-1; **6**-*trans*, 101143-58-2; **6**-*cis*, 84279-69-6; **7**-*trans*, 101143-59-3; **7**-*cis*, 84279-70-9; **8**-*trans*, 101056-18-2; **8**-*cis*, 101398-96-3; **9**-*trans*, 101056-19-3; **9**-*cis*, 101400-28-6; **10**-*trans*, 75058-23-0; **10**-*cis*, 101398-97-4; **11**-*trans*, 101056-20-6; **11**-*cis*, 101312-95-2; **12**-*trans*, 75061-38-0; **12**-*cis*, 101468-30-8; **13**-*trans*·$xC_2H_4Cl_2$, 101056-22-8; **13**-*cis*, 101312-96-3; salprenOH, 3694-33-5; 5-NO_2-saldien, 101079-16-7; 5-NO_2-saldpt, 88389-93-9; 5-NO_2-salaep, 101079-17-8; 5-NO_2-sal-N(1,4,7,10), 101079-18-9; 5-NO_2-sal-N-(1,5,8,12), 101079-19-0; 5-NO_2-sal-N(1,5,9,13), 101079-20-3; N-(1,5,9,13), 4605-14-5; N(1,4,7,10), 112-24-3; N(1,5,8,12), 10563-26-5; dpt, 56-18-8; dien, 111-40-0; aep, 2706-56-1; 1,3-diamino-2-hydroxypropane, 616-29-5; salicylaldehyde, 90-02-8; 5-nitrosalicylaldehyde, 97-51-8.

Supplementary Material Available: Figure 10, showing the KBr pellet infrared spectra of 5-NO_2-sal-N(1,5,8,12) (---) and Mn^{II}[5-NO_2-sal-N-(1,5,8,12)] (—), Figures 11–13 and 17, showing magnetic susceptibility data and least-squares fits for complexes **4**, **5**, **1**, and **9**, respectively, Figures 14a–c and 15a–c, showing X-band powder EPR spectra for complexes **12**, **7**, **6**, **9**, **13**, and **10**, respectively, Figure 16a,b, showing X-band DMF/toluene glass EPR spectra for complexes **10** and **7**, respectively, Tables IX and X, listing analytical data for Schiff base ligands isolated as solids and manganese(II) complexes, respectively, Tables XI–XIII, listing observed and calculated structure factors, final thermal parameters, and hydrogen atomic positional and thermal parameters, respectively, for Mn^{II}[5-NO_2-sal-N(1,5,9,13)]·0.65$CH_2H_4Cl_2$, Tables XIV–XXVII, listing experimental and calculated magnetic susceptibility data, and Tables XXVIII–XXX, listing intermolecular hydrogen contacts, crystallization solvent bond lengths and angles, and deviations of atoms from their least-squares plane, respectively, for Mn^{II}[5-NO_2-sal-N(1,5,9,13)]·0.65$CH_2H_4Cl_2$ (42 pages). Ordering information is given on any current masthead page.

Contribution from the School of Chemical Sciences, University of Illinois, Urbana, Illinois 61801

Atom Transfer and Chelate Fragmentation Reactions of Bis(cyclopentadienyl)titanium Thiophosphoryls[1]

Gregg A. Zank and Thomas B. Rauchfuss*

Received June 28, 1985

The compound $(RCp)_2TiS_4(PAn)_2$ (**1**; RCp = η^5-RC_5H_4, R = H, Me; An = 4-$MeOC_6H_4$) reacts with 1 or 2 equiv of oxygen to give the six- and seven-membered heterocycles $(RCp)_2TiOS_4(PAn)_2$ (**2**) and $(RCp)_2TiO_2S_4(PAn)_2$ (**3**). These reactions appear to involve the dissociation of **1** to give $(RCp)_2TiS_3(PAn)$ and $[AnPS]_3$, followed by the oxygenation of the latter to give $[AnPSO]_n$ and insertion of an AnPSO fragment into $(RCp)_2TiS_3(PAn)$ to give **2**. In a similar way $(RCp)_2TiS_3(PAn)$ adds $[AnPS_2]_2$ to give $(RCp)_2TiS_5(PAn)_2$ (**4**), an all-sulfur analogue of **2**. Compound **4** converts organic carbonyls into thiocarbonyls concomitant with the formation of **2**. The structure of **3** was determined by single-crystal X-ray diffraction. $(CH_3C_5H_4)_2TiO_2S_4(P(C_6H_4OCH_3))_2$ crystallizes in the triclinic space group $P\bar{1}$, with a = 9.458 (3) Å, b = 10.611 (3) Å, c = 15.975 (5) Å, α = 94.96 (2)°, β = 109.34 (2)°, and γ = 105.38 (2)°. With use of 7288 unique reflections with $I > 3.00\sigma(I)$, the structure was solved by direct methods and refined to a final R = 0.037 and R_w = 0.048. The structure consists of a $(MeCp)_2Ti$ moiety incorporated into a seven-membered Ti–O–P(S,An)–S–S–P(An,S)–O ring (each phosphorus atom maintaining a terminal sulfide and an anisole group). The reaction of **1** or **4** with organic carbonyls gives $(MeCp)_2TiO_2S_3(PAn)_2$, which exists as cis and trans isomers.

Introduction

Monoorganophosphorus sulfides have an extensive chemistry and are of considerable importance as synthetic intermediates and reagents.[2] Aryl derivatives of the phosphorus sulfides have been intensively studied, and five structural types are now characterized, three of the formula $[ArPS]_n$[3-5] (n = 3, 4) and two of the formula $[ArPS_2]_n$[4-6] (n = 1, 2). The dimeric compounds $[ArPS_2]_2$ have received the greatest attention because of their utility in organic chemistry,[7] and their transition-metal derivatives have been the

(1) This is the second of a two-part series; for part 1 see ref 10.
(2) Maier, L. *Top. Phosphorus Chem.* **1970**, *2*, 43–131; **1978**, *10*, 129–69.
(3) Cetinkaya, B.; Hitchcock, P. B.; Lappert, M. F.; Thorne, A. J.; Goldwhite, H. *J. Chem. Soc., Chem. Commun.* **1982**, 691–3.
(4) Lensch, C.; Clegg, W.; Sheldrick, G. M. *J. Chem. Soc., Dalton Trans.* **1984**, 723–5.
(5) Lensch, C.; Sheldrick, G. M. *J. Chem. Soc., Dalton Trans.* **1984**, 2855–7.
(6) Appel, R.; Knoch, F.; Kunze, H. *Angew. Chem., Int. Ed. Engl.* **1983**, *22*, 1004–5. Navech, J.; Majoral, J. P.; Kraemer, R. *Tetrahedron Lett.* **1983**, *24*, 5885–6. Yoshifuji, M.; Toyota, K.; Ando, K.; Inamoto, N. *Chem. Lett.* **1984**, 317–8.

0020-1669/86/1325-1431$01.50/0